# UNIVERSITY OF NAPLES "FEDERICO II"

**XXV Course**

**PhD Program in Neuroscience**

**School of Molecular Medicine**

# Effects of bone mesenchymal stem cells (BMSCs) on the rat pial microvascular remodeling after transient middle cerebral artery occlusion and different reperfusion times


**Coordinator:**

**Prof. Lucio Annunziato**

**Tutor:**

**Prof. Antonio Colantuoni**

**PhD student:**

**Daniela Sapio**


**ACADEMIC YEAR 2012-2013**

# INDEX

## *Abstract*

***Background and Purpose -***Transplantation of bone mesenchymal stem cells (BMSCs) represent a potential therapy for ischemic stroke, we sought to evaluate the long-term effects of these cells treatment on rat pial microcirculation after middle cerebral artery occlusion (MCAO).

***Method -*** Male rats were subjected to 2-hours MCAO followed by an infusion of 1 x $10^6$ BMSCs or phosphate-buffered saline into internal carotid artery. Pial microcirculation was observed through a closed cranial window at different reperfusion time (7, 14 and 28 days) by fluorescence microscopy. Geometric characteristics of pial arteriolar networks, permeability increase, leukocyte adhesion, perfused capillary density were analyzed. The expression of the most important proteins in the process of angiogenesis was evaluated by western blot analysis. Finally, we performed green fluorescent protein (GFP)-BMSCs to transplanted to follow their distribution on infarcted area.

***Results -*** The post-ischemic penumbra induced by MCAO is a site of intense microvascular reorganization, characterized by new vessel connections resulting in several anastomotic arterioles. The intracarotid administration of bone mesenchymal stem cells up to 28 days post middle cerebral artery occlusion induced an accelerated pial vascular remodeling. These arcades were likely vessels sprouting from preexistent arterioles localized in the penumbra area, able to place on the ischemic core, accompanied by increased expression of vascular endothelial growth factor and endothelial nitric oxide synthase. GFP-BMSCs showed the distribution and organization in infarcted area up to 28 days of reperfusion.

***Conclusions -*** Pial vascular remodeling after MCAO mainly involves arteriolar networks; the graft of bone mesenchymal stem cells accelerates this processes through angiogenic mechanisms.

# 1. INTRODUCTION

The blood supply to the brain provides it with oxygen, nutrients and a means to excrete metabolic waste. If the blood supply is interrupted in any way, then devastating consequence can ensue. The brain has an intense metabolism, and the capacity for anaerobic metabolism is minimal; interruption of the oxygen supply for a few minutes can cause irreversible damage.

The vascular system is a supporting system, and disease of vascular origin will cause secondary alterations in other neural systems. Vascular disease is often identified by its characteristic temporal profile of sudden onset, with rapid appearance of specific combinations of neurological symptoms. A stroke (´brain attack`) or cerebrovascular accident is characterized by a temporary, or permanent, loss of function of brain tissue caused by interruption of the vascular supply. Stroke is the third leading cause of death after heart disease and cancer. It is most often due to disease or trauma. Brain infarctions account for 75% of strokes, and cerebrovascular accidents such as subarachnoid or intracerebral hemorrhages account for a further 15%. Head injury accounts for about 1% of deaths and up to one-half of road traffic accident-related deaths. It is, like stroke, a common cause of death and disability. Following stroke injury, it is important to identify the type of stroke, minimize the stroke size and evaluate what treatment options are available to either prevent the problem from reoccurring or to maximise recovery of function after the event.

## *1.1 Physiological control of cerebral blood flow*

Brain cells are dependent on aerobic metabolism for their survival; if deprived of oxygen for 20s (anoxia), the brain lapses into unconsciousness as the affected neurons cease electrical activity. This can become irreversible if it extends beyond 5 min. It takes longer for this process to occur in the brainstem and spinal cord. The brain represents approximately 2% of the body weight but uses 20% of the available oxygen and 15% of the cardiac output.

Blood flow is about 750 mL/min, and this remains constant throughout the day, whether we are asleep, awake, lying down or standing up. The average blood flow is 50-55 mL/100g per minute, then ischaemia (lack of bloodborne oxygen) ensues, and infarction (tissue cell death) occurse below 20 mL/100g per minute. Maintaining a constant blood

flow depends on a constant blood perfusion pressure and vascular resistance. The cerebral perfusion pressure is defined as the mean arterial pressure minus the intracranial pressure, rather than cerebral venous pressure. This is because the brain is enclosed within the skull, and it is the pressure within this ´closed box´ that is effectively acting on the outside of the arteries and thus is the one that opposes arterial pressure. The cerebral perfusion pressure does not always remain constant, and as mean arterial pressure is closely regulated within narrow ranges, changes must occur in the cerebral vascular resistance to compensate for changes in perfusion pressure. This occurs through mechanisms intrinsic to the brain: when perfusion pressure decreases, vascular pressure decreases; if perfusion pressure increases, so does the resistance. Cerebral blood flow is kept relatively constant by several processes.

Metabolic mechanisms involve the action of vasodilating agents such as adenosine, $K^+$, $H^+$ and nitric oxide (NO), which regulate arteriole size. Autoregulation is a major homeostatic mechanism whose function is to keep blood flow constant over the pressure range 60-150 mmHg. It is closely related to local metabolic processes, and use chemical and neurogenic mechanisms to control pressure, the most important being the levels of carbon dioxide and oxygen. Hypoxia and hypercarbia cause an increase in cerebral blood flow, whereas hypocarbia causes a decrease in blood flow, by constricting or relaxing the arteriole smooth muscle. These changes are brought about by alterations in the $H^+$ concentration in the extracellular fluid compartment surrounding the blood vessels.

Another source of autoregulation is the level of intraluminal pressure within the arterioles. Any increase in pressure produces a direct, myogenic response that is sufficient to maintain a steady state of perfusion. These processes are not controlled by the sympathetic nervous system, as drugs that effect blood pressure do not, in general, have any effect on cerebral blood flow. Too much oxygen can also have deleterious effects on brain cells. Increased levels of extracellular oxygen can lead to the formation of free radical ions, which can damage brain cells by the process of excitotoxicity.

Free radicals also destabilize neurotransmitters by changing the tissue pH, and causing them to spontaneously oxide, which can further exacerbate the toxicity. Not all areas of the brain are equally active at the same time. Oxygen is shunted around to areas (and cells) that need it most for a particular task at a particular time because they are more metabolically active. For example, there is relatively more blood flow to the motor cortex

when someone is performing a motor task. This suggest that blood is shunted around to whichever area needs it.

A consequence of this is that areas that are not actively processing information have a decreased bood flow. This observation has led to the development of brain scan techniques that measure regional cerebral blood flow to functionally active areas following injection of radioactive isotope of the inert gas xenon ($^{133}$Xe) into an artery. This was the first method used to provide detailed insight into how various brain areas functioned in normal and pathological conditions, because of the direct relationship between blood flow and cellular metabolic activity [1].

### *1.1.1 Blood supply to the brain*

Blood is supplied to the brain via the anterior and posterior circulations. The anterior circulation supplies supratentorial structures (the cortex and diencephalon), whereas the posterior circulation supplies the structures in the posterior fossa (cerebellum and brainstem).

Both circulations initially arise from the aortic arch, but the posterior circulation enters the skull cavity through the foramen magnum, while the anterior circulation enters through the foramen lacerum, to lie within the cavernous sinus.

The anterior circulation carries 80% of the blood supply to the brain. It is derived from the internal carotid arteries (ICAs), which branch off from the common carotid arteries and enter the brain cavity through the carotid canal (in the petrosal and sphenoid bones of the skull) to emerge on its interior surface via the foramen lacerum (which is only visible in a dried skull, as in life it is filled with cartilage). The arteries make a series of stepwise turns, passing through the cavernous sinus, before emerging, on each side, next to the optic chiasm, where they divide into their major branches, the middle cerebral artery (MCA) and anterior cerebral artery (ACA). The two anterior cerebral arteries are connected by the anterior communicating artery. The posterior circulation comprises the vertebral, basilar and posterior cerebral arteries (PCAs), and they convey the remaining 20% of the arterial supply to the posterior fossa brain structures and inferior surface of the posterior aspects of the cortex. The anterior and posterior circulations are connected together at the base of the midbrain around the optic chiasm by a network of arteries called the circle of Willis. The arteries that form the circle of Willis are a single anterior

communicating artery, a pair of ACAs, a pair of ICAs, a pair of posterior communicating arteries and a pair of PCAs. There is a substantial amount of anatomical variation between individuals in the arrangement of this circle, due to developmental changes. During embryonic development, the ICA, supplies the ACA, MCA and PCA, but as the brain develops, the PCA develops from the basilar artery, as the posterior communicating artery atrophies. However, in approximately 20% of people, the embryonic pattern remains and the PCA branches off the anterior circulation. Common variations in the circle of Willis include absence of one or both posterior communicating arteries, origination of the PCAs from an enlarged posterior communicating artery, or multiple small anterior communicating arteries. These anastomoses allow for a certain amount of shunting of blood from the anterior to posterior circulation or from one side to the other in the event of arterial occlusion, but generally the anastomoses are not effective against total occlusion of one the major supply arteries [1].

### *1.1.2 Main terminal branches of the anterior system*

The ICA gives rise to several small branches at its proximal portion before dividing into its two main terminal branches, the MCA and ACA. The hypophysial artery forms a plexus around the pituitary stalk. The ophthalamic artery is the most proximal branch of the ICA. It supplies the orbit, the eye muscles and the retina, and eventually connects to the external carotid (facial and superficial temporal) arteries through anastomoses with arteries of the forehead and nose (ethmoidal, nasal, supraorbital and supratrochlear). Occlusion of the ophthalamic artery is an important diagnostic sign in transient ischaemic attacks.

Another artery that is important in providing anastomoses between different arterial systems is the posterior communicating artery, which links the carotid and vertebral systems. Clinically, this is one of the most frequent sites for aneurysm formation, at the junction where it leaves the ICA. The MCA is the largest and most important branch of the ICA, and receives 80% of the carotid blood flow. Its proximal part gives off three deep branches. The lateral and medial striate arteries supply the striatum and the internal capsule regions of the brain. Occlusion of these deep arteries is the chief cause of classic stroke, and the most common location is the putamen and internal capsule. The anterior choroidal artery supplies parts of the limbic system, the hippocampus and amygdala, in the medial temporal lobe, the posterior part of the internal capsule, the optic radiation and the choroid

plexus of the inferior horn of the lateral ventricle, which is important in the formation of cerebrospinal fluid (CSF). Occlusion of this artery may cause hemiparesis, hemianaesthesia, hemianopsia and loss of short-term memory.

The more distal part of the MCA travels laterally through the lateral fissure and then separates into superior and inferior branches that supply most of the lateral side of the brain (frontal, parietal, temporal and occipital regions). This ramification is known as the middle cerebral candelabra (from angiographic studies). The branches are named with respect to the cortical region that they supply. The ACA supplies the medial side of the frontal and parietal lobes as far back as the parieto-occipital sulcus, and overlaps onto the orbital and lateral surfaces of the brain. It winds around the genu of corpus callosum before dividing into two main terminal branches. The callosomarginal artery supplies the cingulate and frontal gyri and the paracentral lobule. The pericallosal artery supplies the corpus callosum. On the lateral surface of the brain, its branches anastomose with terminal branches of the MCA. The ACA gives off one proximal branch, the recurrent artery of Heubner, which supplies the ventral part of the basal ganglia and the anterior limb of the internal capsule. It anastomoses with the lateral striate arteries of the MCA. Occlusion of this artery is rare but can cause `clumsy hand` syndrome, with contralateral weakness of the arm and face [1].

### *1.1.3 Differentiated properties of brain capillary endothelial cells account for the Blood-Brain Barrier*

Brain microvessels are composed of endothelial cells, pericytes with smooth muscle-like properties that reside adjacent to capillaries, and astroglial processes that ensheath more than 95% of the abluminal microvessel surface. It was originally thought that the glial foot processes formed the blood-brain barrier, but electron-microscopic studies identified the endothelial cell as the principal anatomic site of the blood-brain barrier.

The blood-brain barrier results from specialized properties of the endothelial cells, their intercellular junctions, and a relative lack of vesicular transport. In capillaries of peripheral organs and in the relatively few brain capillaries that do not form a barrier (eg, the circumventricular organs) blood-borne polar molecules diffuse passively across vessels

through spaces between endothelial cells, through specialized cytoplasmic fenestrations, or by fluid-phase or receptor-mediated endocytosis.

Endothelial cells of blood-brain barrier vessels are relatively deficient in vesicular transport. They also are not fenestrated. Instead they are interconnected by complex arrays of tight junctions. These junctions between the endothelial cells block diffusion across the vessel wall. All endothelial cells are interconnected by tight junctional complexes but normally have low resistance (5-10 $\Omega/cm^2$). In the vessels of the blood-brain barrier, however, the resistance is very high (2000 $\Omega/cm^2$), and molecules as small as $K^+$ ions are excluded.

Normal development and brain function require a large number of compounds that must be able to cross brain microvessels. Entry into the CSF is achieved primarily in three ways: (1) by diffusion of lipid-soluble substances, (2) by facilitative and energy-dependent receptor-mediated transport of specific water-soluble substances, and (3) by ion channels.

The brain is separated from blood only by a very large surface of endothelial cell membranes (approximately 180 $cm^2$/ g in gray matter). This permits the efficient exchange of lipid-soluble gases such as $O_2$ and $CO_2$, an exchange limited only by the surface area of the blood vessel and by cerebral blood flow. Barrier vessels are impermeable to poorly lipid-soluble molecules such as mannitol, as compared to very lipid-soluble compounds such as butanol. The permeability coefficient of the blood-brain barrier for many substances is directly proportional to the lipid solubility of the substance as measured by the oil-water partition coefficient.

Most substances that must cross the blood-brain barrier are not lipid soluble and therefore cross by specific carrier-mediated transport systems. Because the brain uses glucose exclusively as its source of energy, the hexose transporter (glucose transporter isotype-1, Glut1) of the blood-brain barrier endothelial cells has been particularly well characterized.

## *1.2 Stroke*

Stroke is a highly disabling neurodegenerative condition with a high incidence in industrialized countries [2].

Stroke is one of the leading causes of death and the most common cause of adult disability. Stroke often causes devastating and irreversible loss of function. There is a wide

range of sensory, motor, and cognitive deficits including tremor, lack of coordination, and partial paralysis. A stroke occurs when the blood supply to part of the brain is suddenly interrupted or when a blood vessel in the brain bursts, spilling blood into the spaces surrounding brain cells. The neuronal cell death associated with cerebral ischemia is due to the lack of oxygen and glucose, and may involve the loss of ATP, excitotoxicity of glutamate, oxidative stress, reduced neurotrophic support, and multiple other metabolic stresses.

Ischemia ultimately leads to *infarction*, the death of brain cells which are eventually replaced by a fluid-filled cavity (or *infarct*) in the injured brain. When blood flow to the brain is interrupted, some brain cells die immediately, while others remain at risk for death. These damaged cells make up the *ischemic penumbra* and can linger in a compromised state for several hours. With timely treatment these cells can be saved. There are two forms of stroke: *ischemic* - blockage of a blood vessel supplying the brain, and *hemorrhagic* - bleeding into or around the brain.

### *1.2.1 Ischemic Stroke*

An ischemic stroke occurs when an artery supplying the brain with blood becomes blocked, suddenly decreasing or stopping blood flow and ultimately causing a brain infarction. This type of stroke accounts for approximately 80 percent of all strokes. Blood clots are the most common cause of artery blockage and brain infarction. The process of clotting is necessary and beneficial throughout the body because it stops bleeding and allows repair of damaged areas of arteries or veins. However, when blood clots develop in the wrong place within an artery they can cause devastating injury by interfering with the normal flow of blood. Problems with clotting become more frequent as people age. Blood clots can cause ischemia and infarction in two ways. A clot that forms in a part of the body other than the brain can travel through blood vessels and become wedged in a brain artery.

This free-roaming clot is called an *embolus* and often forms in the heart. A stroke caused by an embolus is called an *embolic stroke*. The second kind of ischemic stroke, called a *thrombotic stroke*, is caused by *thrombosis*, the formation of a blood clot in one of the cerebral arteries that stays attached to the artery wall until it grows large enough to block blood flow. Ischemic strokes can also be caused by *stenosis*, or a narrowing of the artery due to the buildup of *plaque* (a mixture of fatty substances, including *cholesterol*

and other lipids) and blood clots along the artery wall. Stenosis can occur in large arteries and small arteries and is therefore called *large vessel disease* or *small vessel disease*, respectively. Brain injury following cerebral ischemia involves a complex succession of events that evolve spatially and temporally, causing varying degrees of cell damage depending on the characteristics of the initial insult [3]. The ischemic core and the peri-infarct zone (penumbra) suffer differing degrees of cellular damage [4], and it is widely accepted that cell death in the ischemic core is triggered by necrosis while that which occurs in the penumbra is predominantly mediated by apoptosis [5]. As apoptosis is a reversible process, therapeutic interventions targeting this process have the potential to prevent or limit cell death in the peri-infarct zone, even when applied post-ischemia.

### *1.2.2 Mechanisms of cell injury in ischemic stroke*

The brain has a very high rate of oxidative metabolism. Anaerobic metabolism in the brain is negligible, and as a consequence the brain is extremely vulnerable to hypoxic damage. Cell death occurs in stroke because of anoxia and the resultant loss of ability of the cell to maintain the integrity of the cell membrane through the activity of the energy-dependent ATPase pumps. The pathophysiological consequences of stroke involve a complex sequence of events that involve over time and space and set up several vicious circles that ultimately lead to brain cell death. The main mechanisms involved include excitotoxicity, inflammation and programmed cell death, and molecular pathways for these have been extensively studied. The mechanisms involved are different in different areas of the stroke region: at the site of infarct, the core region, hypoxia is most severe and brain tissue rapidly dies. Surrounding the core is an area called the ischaemic penumbra, where there is residual blood flow and where brain cells undergo potentially reversible electrophysiological and metabolic failure. These cells have not yet entered signal cascades that lead to cell death. The size of the penumbra is variable. The importance of this penumbra is that here the cell damage may be reversible, and those drug treatment that block the release and action of excitotoxins may reduce or limit the amount of functional deficit. When the brain becomes hypoxic, ATP levels start to fall and the ATP-dependent $Na^+$ pumps in the neuronal and glial cell membranes become dysfunctional. The $Na^+$ that enters the cells, either during action potentials or because of the ongoing leaks in the membrane, cannot be pumped out, causing membrane depolarization. This creates an

inward osmotic force, as the influx of $Na^+$ (and $Cl^-$) is much greater than the efflux of $K^+$, and the cells swell due to the passive influx of water, causing oedema. Cells eventually burst as the cell membrane fails; this is necrotic cell death.

The brain is encased in a rigid box, the skull, so if the neurons start to swell, this will increase the intracranial pressure, leading to compression of the ventricles and the cerebral blood vessels. Compression of the blood vessels, expecially the veins, reduces the blood flow and hence further decreases the oxygen supply. A vicious circle is set up that leads to a rapid decline in cerebral perfusion. Brain oedema is one of the earliest events in stroke, and its magnitude is one of the major factors that determine whether the patient will survive beyond the first few hours. The reuptake process that removes glutamate from the synaptic cleft and stabilizes glutamatergic transmission is also energy-intensive, and thus requires ATP. As soon as oxygen levels fall and ATP levels decline, the reuptake process slows down. Consequently, glutamate begins to accumulate in the synaptic cleft and, with the associated rise in extracellular $K^+$, further depolarization of cells may occur. This leads to more hyperexcitability and more glutamate release, and yet another vicious circle.

Activation of the N-methyl-D-aspartate (NMDA) glutamate receptor leads to $Ca^{2+}$ influx into neurons. This receptor is normally tightly regulated by a number of factors, so that $Ca^{2+}$ entry into neurons is closely controlled. Excessive extracellular glutamate levels lead to prolonged neuronal depolarisation via 4-amino-3-hydroxy-5-methyl-4-isoxazole propionic acid (AMPA) receptors, which in itself is not harmful. However, the depolarisation of the postsynaptic cell also activates the NMDA receptor (which is held inactive at normal resting potentials by a $Mg^{2+}$ block of the receptor), which in turn leads to further $Ca^{2+}$ entry. This is where critical processes are triggered, due to $Ca^{2+}$ overload as the $Ca^{2+}$ buffering systems of neurons, the mitochondria and endoplasmic reticulum, fail.

The rise in internal $Ca^{2+}$ level activates many second messenger systems, which all demand energy in the form of ATP or other substrates.

However, because of hypoxia, this energy is not available. Disruption of neuronal $Ca^{2+}$ -induced processes leads to the formation of free radicals, such as the superoxide anion ($O^{2-}$), via the activation of NO production. These free radicals are very reactive and initiate cell damage by reacting with many cell components (e.g. lipid peroxidation reaction). This eventually damages the cell so badly that it undergoes necrosis. Thus, glutamate toxicity is a prominent cause of necrotic cell death [1].

### *1.2.3 Animal Model of Stroke*

Development of effective stroke therapy requires use of animal models that can simulate human pathology in a reproducible and physiologically relevant manner.

Currently, the intraluminal suture model of MCAO has been widely used to induce ischemic brain lesions. As the MCA is occluded via a cervical carotid approach, this obviates the requirement for a craniectomy and the associated problems with opening the skull. However, the lesions caused by the MCAO tend to be variable in size; in addition, animals have been excluded from analysis by arbitrary criteria such as unexpected behavior in most series. The development of reliable and reproducible animal models for cerebral ischemia is needed for the systematic study of the pathophysiology and treatment of stroke.

### *1.2.4 Stroke treatment and neuroprotection*

The majority of neuroprotective treatments for cerebral ischemia have been efficacious in experimental studies but have failed their clinical trials.

Only i.v. thrombolysis (rtPA) has been shown to be effective; however its narrow therapeutic time window makes it a treatment for a reduced percentage of patients [6]. In the past, protective therapies have been directed towards saving neural cells. Stroke induced damage compromises the integrity of the neurovascular unit [7] through various pathophysiologic mechanisms. Angiogenesis, neurogenesis and synaptogenesis are interrelated mechanisms that promote brain plasticity and help to repair the neurovascular unit and recover neurological function [8]. Endogenous brain plasticity can be stimulated by rehabilitation, stimulation and/or administration of trophic factors and cell therapy. The different cell lines used in experimental stroke models include embryonic, hematopoietic and mesenchymal stem cells (MSCs) [9]. The advantages of MSCs include their multipotency, which facilitates *in vitro* and *in vivo* tissue repair [10], and their ease of isolation, which allows immediate availability for clinical application.

## *1.3 MSCs*

The transplantation of stem cells may repair injured nervous tissue through replacement of damaged cells, hence providing an effective treatment for brain diseases.

Stem cells are well known for the self-renewing capacity and multipotential nature like high differentiation and "homing" capability, which provides the solid foundation of treatment for various diseases. Different populations of adult stem cells that can contribute to the regeneration of muscle, liver, heart and vasculature have been described, although the mechanisms by which this is accomplished are still not completely understood, (Fig. 1) [11]. Several types of stem cells have been transplanted into the injured brain, including mesenchymal stem cells (MSCs) [12–13]. Multipotent mesenchymal stem cells (MSCs) are in the centre of a rapidly moving field in rheumatology, initially based on their cartilage/bone differentiation potential now partly eclipsed by their capacity to counteract adverse host immune responses, improve angiogenesis and prevent fibrosis. MSCs are characterized by their capacity to adhere to plastic, their phenotype are $CD90^+$, $CD73^+$, $CD105^+$, absence of haematopoietic markers including $CD45^-$, $CD11b^-$, $CD14^-$ and $HLA\text{-}DR^-$. MSCs have been found to produce improvements in disease models, although a limited number of the cells could be demonstrated to be stably engrafted. The injected mesenchymal stem cells home to the injured area, in particular to hypoxic, apoptotic or inflamed areas, and release trophic factors that hasten endogenous repair [11]. The basic theory of stem cell therapy is that stem cells would replace injured cells, which seems to be a part of theories in the treatment for brain diseases.

However, other mechanisms are proposed, including the possibility that stem cells may release or stimulate release of trophic factors which would be neuroprotective, enhance angiogenesis, inhibit fibrosis and apoptosis, and stimulate recruitment, retention, proliferation and differentiation of tissue-residing stem cells [11].

Their efficacy may rely on the collaboration of secretion of cytokines and direct differentiation. It has been demonstrated that MSCs can promote functional recovery by producing trophic factors that induce survival and regeneration of host neurons [14].

Besides the neurotrophic factors, MSCs can produce the extracellular matrix molecules that can support neural cell attachment, growth and axonal extension [15]. Several studies have proved that MSCs can be induced to express neural markers in vitro [16, 17], while after stem cells migrating in the brain, some new neurons in the adult human hippocampus have been found [14, 18, 19]. There is no precise definition of mechanisms of stem cell - based therapy for brain diseases yet; however, as beneficial effects have been demonstrated, details inside cell therapy need further investigation. In

addition to the advanced research into the precise mechanisms, strategies should also be established to enhance the homing capability of MSCs towards brain lesions for better therapeutic effects as well as reducing side effect.

Over the past 20 years, stem cell technologies have become an increasingly attractive option to investigate and treat brain diseases.

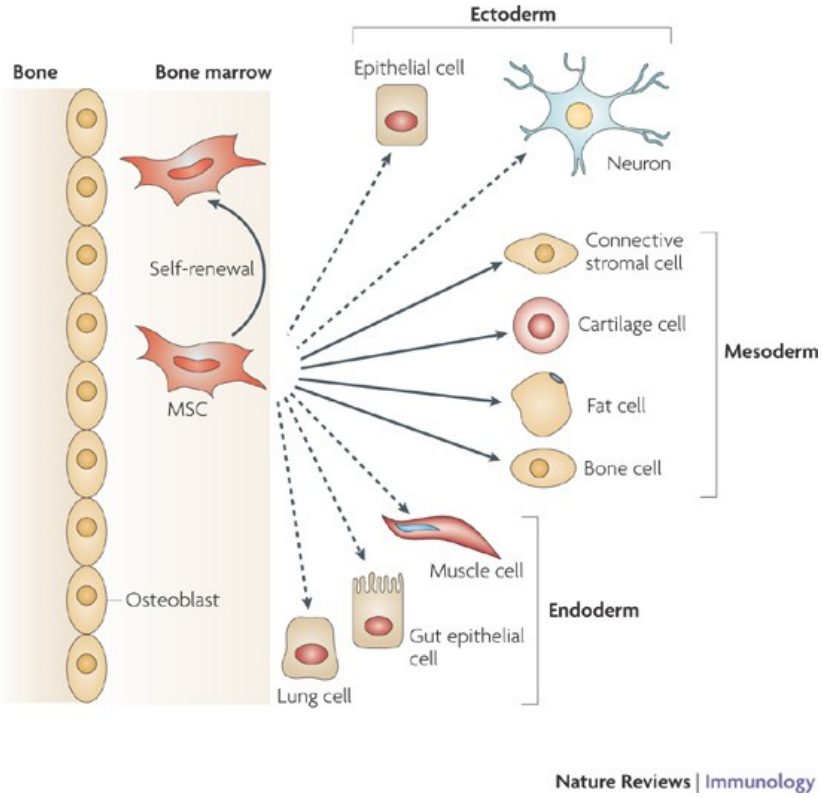


**Figure 1:** this figure shows the ability of mesenchymal stem cells (MSCs) in the bone-marrow cavity to self-renew (curved arrow) and to differentiate (straight, solid arrows) towards the mesodermal lineage. The reported ability to transdifferentiate into cells of other lineages (ectoderm and endoderm) is shown by dashed arrows, as transdifferentiation is controversial *in vivo*.

### *1.3.1 BMSCs for the treatment of ischemic stroke*

There is an urgent need to remodel the injured brain to improve neurological outcome after ischemic stroke. Stem cell-based therapy may provide a method to achive this (20, 21).

Bone mesenchymal stem cells (BMSCs) can be easly obtained from patients themselves without ethical or immunological problems and can proliferate massively *in vitro* (Fig. 2).

Under certain conditions, BMSCs can be induced to differentiate into multiple cell types, including neurons (22, 23) and endothelial cells (24). Ischemic stroke causes a disturbance of neuronal circuitry and disruption of the blood–brain barrier that can lead to functional disabilities, which is the most important vascular central nervous system disorder that remains a leading cause of death and disability [25]. BMSCs have great potential as therapeutic agents in stroke management, since they are easily obtained from bone marrow and can be expanded rapidly ex vivo for autologous transplantation [26]. Increasing evidences suggest that BMSCs can be used to treat stroke with satisfactory results, as BMSCs can migrate to the ischemic areas, secrete some trophic factors. After middle cerebral artery occlusion (MCAO), BMSCs that are administered by different routes and applied for different time of treatment all show promising therapeutic effects.

The three major routes of BMSCs administration are intrastriatal, intracarotid, and intravenous injection. BMSCs intend to migrate to the region of the ischemic hemisphere than to the contralateral non-ischemic hemisphere, and make contribution to the functional recovery [27, 28]. Transplanting BMSCs after MCAO has been found significantly improving neurological functional recovery, as well as promoting endogenous neurogenesis and reducing apoptosis. However, gene modification is always a promising way to enhance therapeutic benefits. Rats with ischemic stroke due to MCAO that received fibroblast growth factor-2 (FGF-2)-modified BMSCs or BDNF-modified BMSCs had a significantly reduced infarction volume 14 days after MCAO [29, 30].

Other combination methods have also been studied and showed great therapeutic benefits, which demonstrates that BMSCs have great potential in stroke treatment. Transplanting a composite graft of fresh bone marrow along with brain-derived neurotrophic factor (BDNF) into the ischemic boundary zone (IBZ) of rat brain can facilitate BM cells to survive and differentiate, and improves functional recovery after middle cerebral artery occlusion (MCAO) [31].

Transplanting BMSCs increased expression of brain-derived neurotrophic factor (BDNF) [32], nerve growth factor (NGF) [27,32], vascular endothelial growth factor (VEGF) [33], basic fibroblast growth factor (bFGF) and so on. These trophic factors function in the processes of induction of angiogenesis, neurogenesis and neuroprotection, and it seems that these factors/cytokines secreted by BMSCs play most important role in functional recovery after MCAO.

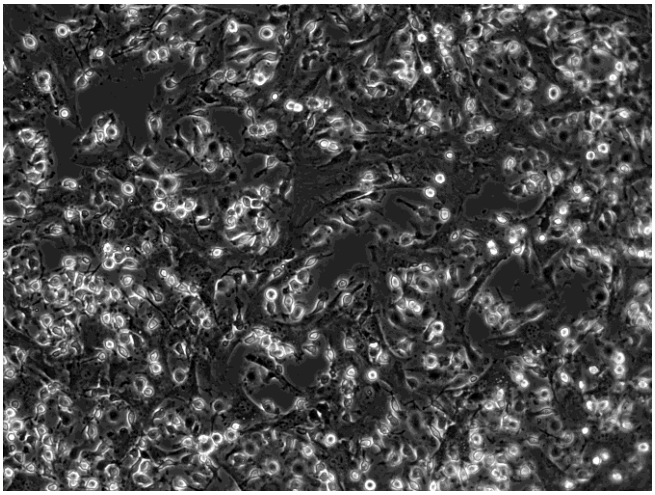

**Figure 2**: culture of bone mesenchymal stem cells

# 2. AIM

Cerebral stroke has been studied in several experimental models, where particular attention has been devoted to neuronal dysfunctions, metabolic events and vascular involvement [34, 35, 36]. Most of studies, however, have been focused on neuronal damage, while no angiogenesis has been documented in areas near the ischemic core, such as the necrotic area induced by middle cerebral artery occlusion (MCAO) [37]. Bone marrow mesenchymal stem cells (BMSCs), a heterogeneous population of plastic-adherent cells, have been used for the treatment of experimental stroke [38]. After ischemia breakdown of the blood-brain barrier (BBB) is well known; in normal rat brain parenchyma, the integrity of the BBB, it has been demonstrated, using Evans blue extravasation, while intense blue was observed in the infarcted lesion at 7, 14 and 28 days after MCAO [39]. On the other hand, BMSCs migrate selectively into damaged brain areas after intravenously injection at an early phase after ischemia [40, 41]. Specific molecular signals, such as stromal cell-derived factor-1 (SDF-1/CXCR4) intracellular signalling, adhesion molecules and proteases were involved in the interaction of BMSCs to reach, recognize, and function in cerebral ischemic tissue [40]. BMSCs have an inhibitory effect on T-cell proliferation triggered by cellular or humoral stimuli [42], while under specific conditions, BMSCs can be induced to differentiate *in vitro* into multiple cell types, including neurons [43, 44] and endothelial cells [45]. The ability to form capillaries in semisolid medium was tested with an in vitro angiogenesis kit; the cells were cultivated in the absence or in the presence of two different concentrations of VEGF. Furthermore, when cultured in presence of endothelial growth supplements, the cells start to express endothelial markers [46]. Kinnaird et al. have shown that mesenchymal stem cells express a wide spectrum of angiogenic growth factors and may stimulate collateral vessel formation by paracrine mechanisms after the injection of these cells into the adductor muscles of the ischemic hindlimb. They found that local production of bFGF and VEGF increased in BMSC-injected tissue and documented colocalization of BMSCs and VEGF [47].

One of the most important questions for a follow-up cell therapy study is the ultimate fate of the cells to evaluate whether *in vivo* these cells are capable to accelerate the physiological mechanism of remodeling. Therefore, we observed the pial networks at various time points after induction of MCAO to study BMSCs potential therapeutic

benefits to generate blood vessels, evaluating geometric characteristics of pial arterioles as well as microvascular permeability, leukocyte adhesion to venular walls and capillary perfusion. We correlated these vascular observations with the determination of VEGF, eNOS, nNOS and iNOS expression to clarify their role during pial arteriolar network reorganization [48].

Moreover, in this study, we performed *in vivo* green fluorescent protein (GFP)-BMSCs to transplanted to follow their distribution on infarcted area.

# 3. MATERIALS AND METHODS

All experiments were conducted according to the *Guide for the Care and Use of Laboratory Animals* published by the US National Institutes of Health (NIH Publication No. 85-23, revised 1996) and to institutional rules for the care and handling of experimental animals. The protocol was approved by the "Federico II" University of Naples Ethical Committee.

## *3.1 Isolation and identification of BMSCs and GFP-BMSCs*

The BMSCs and GFP-BMSCs were isolated under sterile conditions from 8–10 week-old male Wistar rats and transgenic rats expressing the enhanced green fluorescent protein (GFP), respectively, as described previously [49, 50]. Rats were killed by cervical dislocation, and marrow was aspirated from femurs and tibiae for cultivation in DMEM (Dulbecco's Modified Eagle's Medium) supplemented with 10% FBS (fetal bovine serum), 100 U/mL penicillin G. About 13 x $10^6$ whole marrow cells were placed in 150-$cm^2$ tissue culture flasks that were coated with collagen I (Sigma Aldrich). After 5 days, the non-adherent hematopoietic cells were removed by changing the medium. The culture medium was replaced two to three times a week (figure 1). As the culture approached confluence, the cells were detached with 0.05% Trypsin and subcultured. Previous studies showed that the cultured BMSC highly express CD90, CD44, CD105 and CD166, but not CD34 and CD45 [51, 52].

The cells harvested at 3-5 passages were used as BMSCs grafts.

## *3.2 Experimental groups*

Rats were randomly divided into: a) sham-operated animals (S group, n=9) that received the same procedures as the other experimental groups without MCAO; b) ischemic group, submitted to 2 hours MCAO and receiving 300 µl cell-free phosphated buffer saline (PBS) solution, the animals were observed after 1 hour (C1hR group, n=9), 7 days (C7R group, n=9), 14 days (C14R group, n=9) and 28 days (C28R group, n=9) of reperfusion. c) BMSCs-treated group subjected to 2 hours MCAO and the infusion of BMSCs (300 µl PBS solution containing 1 x $10^6$ cells) and observed at: 7 days (BMSCs7R group, n=9), 14 days (BMSCs14R group, n=9) and 28 days (BMSCs28R group, n=9) of reperfusion. d) GFP-BMSCs-treated group was subjected to 2 hours MCAO and the

infusion of 1 x $10^6$ GFP-BMSCs; as controls, the rats were studied after 7 (GFP-7R, n=5), 14 (GFP-14R, n=5) and 28 days (GFP-28R, n=5) of reperfusion.

### *3.3 Animal Model*

Adult male Wistar rats (Charles River) weighing 250-300 g were used. MCAO was induced by intraluminal filament technique as previously described [53]. In brief, rats were anesthetized with intraperitoneal alpha-chloralose (60 mg/kg b.w.), the left common carotid artery (CCA), external carotid artery (ECA) and internal carotid artery (ICA) were exposed.

Subsequently, the ECA was cut with microscissors and heparinised 4-0 nylon filament was inserted into stump of ECA and advanced into ICA about 20 mm until it blocked the origin of the left middle cerebral artery. To determine the perfusion decrease during MCAO, microvascular blood flow was measured by laser Doppler perfusion monitoring (LDPM) on the skull of all animals by a Perimed PF5001 was flowmeter, using a probe (407; Perimed, Sweden) attached to the bone. The sampling rate was 32 Hz and blood flow was expressed as Perfusion Units (PU). After 2 hours occlusion, the filament was withdrawn and 1 x $10^6$ BMSCs or GFP-BMSCs in treated groups or cell-free PBS in control group was infused by insertion of a catheter, immediately the incision was sutured.

Successively, the rats were allowed to recover from surgical intervention with free access to pellets and water. After 1 hour, 7, 14 and 28 days of reperfusion the animals were re-anesthetized, intubated and mechanically ventilated with room air and supplemental oxygen. A catheter was placed in the left femoral artery for arterial blood pressure recording and blood gases sampling, another one was placed in the right femoral vein for injection of the fluorescent tracers [fluorescein isothiocyanate bound to dextran, molecular weight 70 KDa (FD 70), 50 mg/100g b.w. i.v. as 5% wt./vol solution in 5 min, and rhodamine 6G to label leukocytes 1 mg/100g b.w. in 0.3 mL] and for additional anaesthesia. Blood gas measurements were carried out on arterial blood samples withdrawn from arterial catheter at 30 min time period intervals (ABL5; Radiometer, Copenhagen, Denmark). Mean arterial blood pressure (MABP), heart rate, respiratory $CO_2$ and blood gases values were recorded and maintained stable within physiological ranges. Rectal temperature was monitored and preserved at 37.0 ± 0.5°C with a heating pad, where the rats were secured.

To observe pial microcirculation, a closed cranial window (4 x 5 mm) was implanted above the left parietal cortex (posterior 1.5 mm to bregma; lateral, 3 mm to the midline) [54]. The dura mater was gently removed and a 150 μm-thick quarz microscope coverglass was sealed to the bone with dental cement. The window inflow and outflow were assured by two needles secured in the dental cement of the window so that the brain parenchyma was continuously superfused with artificial cerebrospinal fluid (aCSF). The rate of superfusion was 0.5 mL/min controlled by a peristaltic pump. During superfusion the intracranial pressure was maintained at 5 ± 1 mmHg and measured by a Pressure Transducer connected to a computer. The composition of the aCSF was: 119.0 mM NaCl, 2.5 mM KCl, 1.3 mM $MgSO_4 \cdot 7H_2O$, 1.0 mM $NaH_2PO_4$, 26.2 mM $NaHCO_3$, 2.5 mM $CaCl_2$ and 11.0 mM glucose (equilibrated with 10 % $O_2$, 6 % $CO_2$ and 84 % $N_2$; pH 7.38 ± 0.02). The temperature was maintained at 37.0 ± 0.5°C [55].

### *3.4 Fluorescence microscopy and microvascular parameter assessment*

Pial microcirculation was visualized with a fluorescence microscope, as previously reported [57]. The arteriolar network was mapped by stop-frame images and pial arterioles were classified according to a Strahler method, modified according to diameter [56]. The arterioles were classified from the smallest ones, assigned order 1, that gave origin to capillaries (order 0), up to the largest arterioles in the preparations, assigned order 5. When two vessels of the same order joined, the parent vessel was assigned the next higher orders.

If two daughter vessels were of different orders, the parent vessel retained the higher of the two orders. The procedure of the pial arteriole classification was previously described [57].

Moreover, a "connectivity matrix" was calculated to clarify the number and order of daughter arterioles spreading from parent vessels. Briefly, order *n* vessels may spring from orders *n* + 1, *n* + 2, …. vessels, the component of which in row *n* and column *m* was the ratio of the total number of elements of order *n* sprung from elements in order *m* [57].

The increase in permeability was calculated as normalized grey levels (NGL): NGL = (I – Ir)/Ir, where Ir is the average baseline grey level at the end of vessel filling with fluorescence (average of 5 windows located outside the blood vessels with the same windows being used throughout the experimental procedure), and I is the same parameter at the end of reperfusion. Grey levels ranging from 0 to 255 were determined by the MIP

Image program in five regions of interest (ROI) measuring 50 $\mu m^2$ (10x objective). The same location of ROI during recordings along the microvascular networks was provided by a computer-assisted device for XY movement of the microscope table.

Adherent leukocytes (i.e., cells on vessel walls that did not move over a 30-second observation period) were quantified in terms of number/100 μm of venular length (v.l.)/30s using higher magnification (32x, microscope objective). In each experimental group forty five venules were studied. The perfused capillary density (PCD) was measured by computerized method (MIP Image, CNR, Pisa) in an area of 150 $\mu m^2$ and expressed as $cm/cm^2 = cm^{-1}$.

The single pial venule (SPV) blood flow, Q, was calculated according to the following equation: $Q = \alpha \times V_{CL} \times A$, where $\alpha$ was a constant, related to the vessel diameter, $V_{CL}$ was the red blood cell centerline velocity and A was the cross-sectional area. SPV blood flow (SBF) was calculated in venules with diameter of 30-40 μm in both left and right hemisphere. In rats subjected to MCAO and reperfusion, SBF in affected hemisphere was compared with that in contralateral hemisphere. Previous data indicate that single pial venule blood flow may be an accurate measure of pial blood flow drainage from cerebral cortex, because it represent about 30-60% of cortical blood flow. Therefore, we chose to measure single pial venule blood flow to compare with laser Doppler perfusion monitoring data and to estimate the difference in perfusion between affected and non affected hemisphere.

MABP (Viggo-Spectramed P10E2 trasducer – Oxnard, CA – connected to a catheter in the femoral artery) and heart rate were monitored with a Gould Windograf recorder (model 13-6615-10S, Gould, OH, USA). Data were recorded and stored in a computer. Blood gas measurements (arterial partial pressure of $O_2$ and $CO_2$ and pH) were carried out on arterial blood samples withdrawn from arterial catheter at 30 min intervals (ABL5; Radiometer, Copenhagen, Denmark).

## *3.5 Western blotting analysis*

Proteins were extracted from cortex and striatum tissues, and its concentration was determined using the Bio-Rad protein assay kit. Equal amounts of proteins were separated by SDS-PAGE under reducing conditions, and then transferred to polyvinylidene difluoride membranes (PVDF, Invitrogen). The immunoblot was blocked, incubated with

specific antibodies at 4°C overnight, washed and then incubated with a 1:2,000 dilution of HRP (horseradish peroxidase)-conjugated IgG secondary antibody (GE-Healthcare, UK).

Blots were washed again and visualized by ECL system (GE-Healthcare, UK). The optical density of the bands was determined by Chemi Doc Imaging System (Bio-Rad). By incubating PVDF membrane in parallel with Tubulin antibody (1:5,000), normalization of results was obtained.

Specific antibodies were: mouse monoclonal anti-VEGF (1:200), rabbit polyclonal anti-eNOS (1:500), rabbit polyclonal anti-phosphorilated eNOS (Ser 1177) (1:250), mouse monoclonal anti nNOS (1:1000) and rabbit polyclonal anti iNOS (1:500). Antibodies were purchased from Santa Cruz Biotechnology, Santa Cruz, CA, USA.

### *3.6 Quantification of GFP-cells*

To quantify the number of bone mesenchymal stem cells expressing the enhanced green fluorescent protein (GFP-BMSCs) injected after MCAO, we analyzed forty representative stop-frame images (20x objective) per animal. We calculated fluorescent cells located in the interstitium and into the vessels wall to clarify the distribution in the infarcted area. The distribution of these cells in the pial surface, was calculated as number of cells localized in the total infarcted area, considering the same uniform distribution for the entire thickness of the lesion.

### *3.7 Neurological assessment*

All animals were subjected to a battery of behavioural tests before MCAO and at different reperfusion time, using a modified neurological severity score, as previously described by Chen and coworkers [58].

### *3.8 Statistical analysis*

All data were expressed as mean ± SEM. Data were tested for normal distribution with the Kolmogorov-Smirnov test. Parametric (Student's t tests, ANOVA and Bonferroni post hoc test) or nonparametric tests (Wilcoxon, Mann-Whitney and Kruskal-Wallis tests) were used; nonparametric tests were applied to compare diameter and length data among

experimental groups. The statistical analysis was carried out by SPSS 14.0 statistical package. Statistical significance was set at $p<0.05$.

# 4. RESULTS

In sham-operated animals pial arteriolar networks showed the same geometric characteristics when observed in both parietal hemispheres. Pial arterioles, seldom organized in arcading vessels, were classified according to diameter, length and branching. Order 0 was assigned to the capillaries; subsequently, the terminal arterioles were assigned order 1 (mean diameter: 15.5 ± 0.7 μm) and the vessels upstream were assigned progressively higher orders (mean diameter: 23.0 ± 0.5 μm, 34.0 ± 0.6 μm and 44.5 ± 0.7 μm for order 2, 3 and 4, respectively) (table 1).

| **Order** | **Arteriole** N | **Diameter** μm | **Lenght** μm | **Rats** |
|---|---|---|---|---|
| 5 | 10 | 63.0 ± 0.4* | 1.169 ± 420 | 9 |
| 4 | 27 | 44.5 ± 0.7* | 987 ± 250 | 9 |
| 3 | 78 | 34.0 ± 0.6* | 481 ± 120 | 9 |
| 2 | 113 | 23.0 ± 0.5* | 360 ± 100 | 9 |
| 1 | 109 | 15.5 ± 0.7* | 140 ± 83 | 9 |

**Table 1.** Diameter and length of each arteriolar order in sham operated group.

Data obtained from S group were pooled; the diameter (a), length (b) and branching distribution (c) in successive orders of arterioles obeyed Horton's law, according to the following equations:

(a) $Log_{10}D_n = a + bn$

(b) $Log_{10}L_n = a + bn$

(c) $Log_{10}N_n = a + bn$

where a and b are 2 constants. The logarithm of diameter, length and branching was directly proportional to vessel order number. Diameter, length and branching ratios, calculated from the slope of curves, were 1.39, 1.70 and 1.62, respectively.

The branching vessels in the pial networks were described by connectivity matrix indicating vessel connection of one order to another. Usually an order 4 arteriole gave origin to most order 3 vessels (table 2a).

Blood brain barrier integrity was preserved in all sham-operated animals and leukocyte adhesion was not detected (table 3). PCD was 106.1 ± 2.3 $cm^{-1}$ (table 3). All venular vessels were perfused (Fig. 3A, table 3).

### *4.1 MCAO plus 1 hour of reperfusion*

Affected hemisphere presented an ischemic core devoid of blood flow, because all core vessels were not visualized by fluorescent dextran; penumbra area was characterized by reduced blood flow (Fig. 3B). Pial microvasculature was markedly compromised; therefore, no vessel geometric evaluation was performed. Penumbra microvascular permeability was marked as well as leukocyte adhesion (table 3). PCD was reduced to 62.0 ± 1.4 $cm^{-1}$ ($p<0.01$ vs. S group).

Few perfused large venules were detected in affected hemisphere penumbra compared with contralateral ones, where no changes in arteriolar, capillary and venular architecture and blood flow were observed.

### *4.2 MCAO plus 7, 14 and 28 days of reperfusion*

After 7 and 14 days of reperfusion, arterioles gradually increased in number and length; at 28 days of reperfusion, pial arteriolar networks regained diameter ratio as in sham-operated group, but length and branching ratios were higher and lower, respectively. Pial networks were characterized by arcading anastomotic arterioles overlapping the necrotic core.

These vessels appeared at 7 days of reperfusion and were progressively longer (Fig.3C); in C28R their number was the highest compared to all previous ischemic groups (Fig.3G). Order 2 and 1 anastomotic arterioles gave origin to order 2 and 1 vessels (table 2d).

Connectivity matrix indicates that order 4 arterioles were mainly connected to most order 2 vessels in C7R and C14R groups (table 2b, 2c). Order 4 arterioles gave origin to most order 3 vessels only in C28R group (table 2d).

Microvascular permeability progressively decreased in C7R, C14R and C28R groups (table 3). The same time-dependent changes were observed for leukocyte adhesion, progressively decreasing according to increasing reperfusion time. Conversely, PCD gradually increased, up to 28 days of reperfusion (85.0 ± 1.2 cm-1, $p< 0.01$ vs. S group),

(table 3). Venular networks were characterized by progressive increase in number of perfused vessels from 7 days of reperfusion up to 14 days of reperfusion when the number of perfused vessels was in the same range as in contralateral pial microcirculation. At 28 days of reperfusion venules were comparable in number with those observed in S group.

The physiological parameters such as hematocrit, MABP, heart rate, pH, $PCO_2$ and $PO_2$ did not change in the different experimental groups.

### *4.3 MCAO plus BMSCs after 7, 14 and 28 days of reperfusion*

BMSCs, injected after MCAO, were able to accelerate the remodeling processes. After 7 and 14 days of reperfusion, BMSCs stimulated a complex geometric pial networks compared with the respective groups of ischemic rats not treated with BMSCs (Fig. 3D, 3F). Asymmetry was greater in larger vessels, as confirmed by the connectivity matrix showing that vessels of greater orders did not give rise to vessels of the order immediately lower, as reported in sham operated animals and in contralateral hemisphere (table 2e, 2f, 2g). Interstitial edema quantified by the fluorescent dextran outside of vessels, at 7 and 14 days is low when compared with the corresponding groups not treated with BMSCs (0.26 ± 0.03 NGL vs 0.47 ± 0.02 C7R e 0.18 ± 0.04 NGL vs 0.40 ± 0.03 C14R, respectively).

The number of adherent leukocytes after 7 and 14 days was 4.0 ± 0.3 and 3.0 ± 0.4/ 100 μm venular length/30s, respectively ($p<0.01$ vs baseline and C7R and C14R). The capillary density took on a value greater compared to untreated groups (78 ± 1.5 cm/cm$^2$ vs 67 ± 1.0 cm/cm$^2$ CR7, 90 ± 1.2 cm/cm$^2$ vs 70 ± 1.4 cm/cm$^2$ C14R), (table 3). In BMSCs28R group, the animals showed recovered pial networks with anastomotic vessels overlapping the ischemic core (Fig. 3H).

The characteristics of the different orders of vessels described by the connectivity matrix followed the same trend as observed in sham operated animals. The order 4 originated mostly vessels of order 3 and 2, few of order 1 and no capillaries. Vessels of order 3 gave rise to most vessels of order 2, few of order 1 and no capillaries. The vessels of order 2 originated many vessels of order 1 and finally, the vessels of order 1 gave origin to most capillaries (Table 2g).

Indeed, microvascular permeability and leukocyte adhesion were decreased, capillary density was significantly increased more than in sham operated animals (table 3).

The physiological parameters such as hematocrit, MABP, heart rate, pH, $PCO_2$ and $PO_2$ did not change in the different experimental groups.

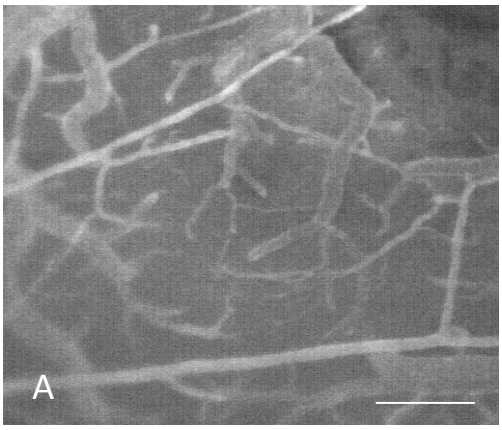
A

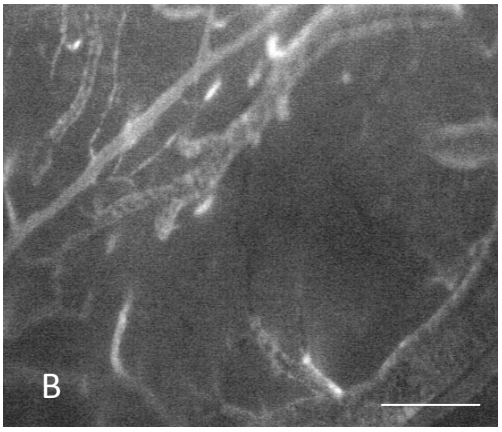
B

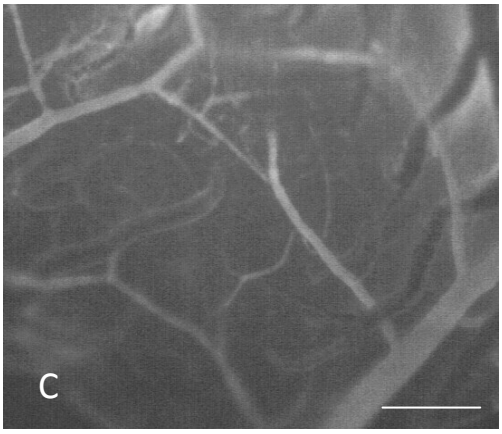
C

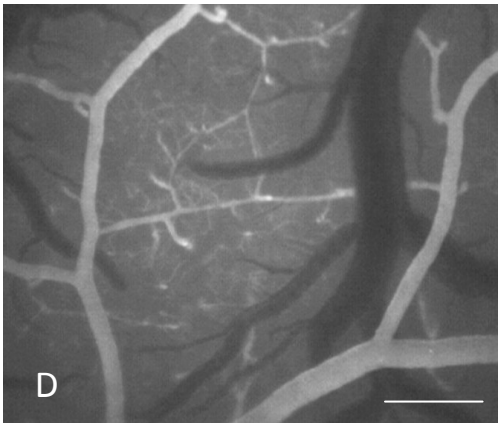
D

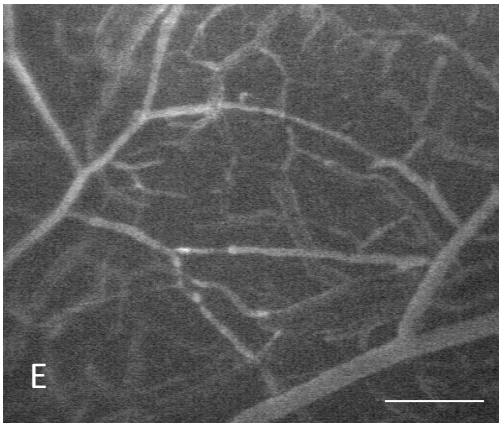
E

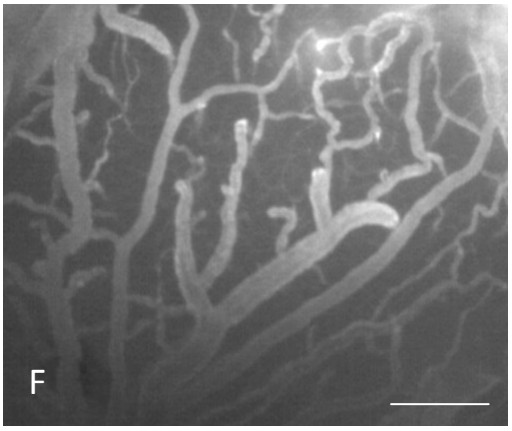
F

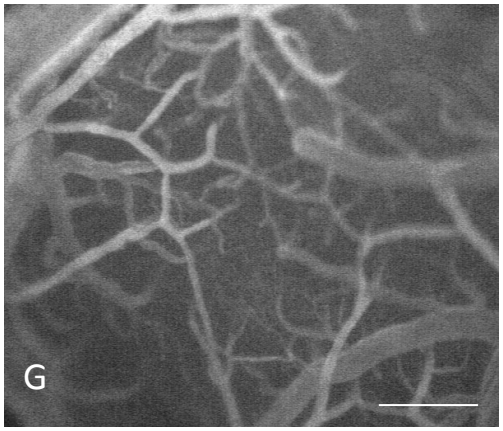
G

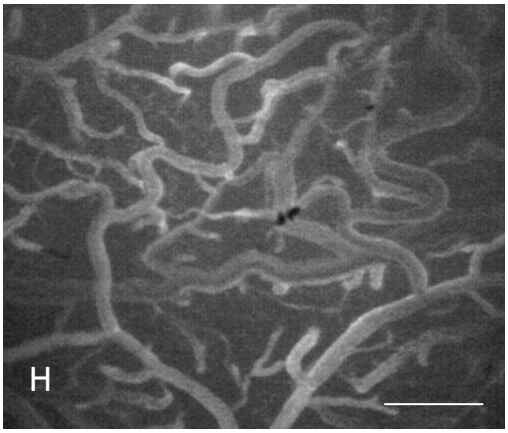
H

**Figure 3.** Computer-assisted image of a rat pial microvascular network in sham operated animals (A), after two hours MCAO and 1 hour (C1hR group) (B), 7days (C7R group) (C), 14 days (C14R group) (E) and after 28 days of reperfusion (G). In treated group (D), after two hours MCAO plus BMSCs and 7 days (BMSCs7R group) (D), 14 days (BMSCs14R group) (F) and 28 days (BMSCs28R group) (H) of reperfusion.
Scale bar = _____ 100 μm.

| Order n | Order m | | | |
|---|---|---|---|---|
| | **1** | **2** | **3** | **4** |
| 0 | 2.28 ± 0.40 (89) | 0.23 ± 0.15 (7) | 0 | 0 |
| 1 | 0.21 ± 0.11 (8) | 2.06 ± 0.54 (64) | 0.65 ± 0.18 (17) | 0.49 ± 0.11 (5) |
| 2 | 0 | 0.25 ± 0.10 (8) | 1.79 ± 1.00 (46) | 1.43 ± 0.70 (14) |
| 3 | 0 | 0 | 0.40 ± 0.16 (10) | 2.50 ± 0.90 (25) |
| 4 | 0 | 0 | 0 | 0.15 ± 0.08 (1) |

| Order | N |
|---|---|
| 4 | 10 |
| 3 | 26 |
| 2 | 31 |
| 1 | 39 |

N: number of vessels studied for each order

**Table 2a**: connectivity matrix of pial arterioles in Sham operated group

| Order n | Order m | | | |
|---|---|---|---|---|
| | 1 | 2 | 3 | 4 |
| 0 | 1.94 ± 0.30 (45) | 0.70 ± 0.09 (13) | 0 | 0 |
| 1 | 0.38 ± 0.14 (9) | 0.89 ± 0.13 (16) | 1.27 ± 0.25 (25) | 0.31 ± 0.11 (2) |
| 2 | 0 | 0.62 ± 0.17 (11) | 0.25 ± 0.12 (5) | 1.55 ± 0.42 (11) |
| 3 | 0 | 0 | 0.36 ± 0.13 (7) | 0.20 ± 0.08 (1) |
| 4 | 0 | 0 | 0 | 0 |

| Order | N |
|---|---|
| 4 | 7 |
| 3 | 20 |
| 2 | 18 |
| 1 | 23 |

N: Number of vessels studied for each order

**Table 2b**: connectivity matrix of pial arterioles in C7R group

| Order n | Order m | | | |
|---|---|---|---|---|
| | 1 | 2 | 3 | 4 |
| 0 | 2.43 ± 0.32 (73) | 1.12 ± 0.11 (21) | 0 | 0 |
| 1 | 0.45 ± 0.12 (13) | 0.94 ± 0.29 (18) | 1.86 ± 0.13 (41) | 0.48 ± 0.20 (4) |
| 2 | 0 | 0.35 ± 0.15 (7) | 0.54 ± 0.12 (12) | 1.77 ± 0.21 (16) |
| 3 | 0 | 0 | 0.60 ± 0.22 (13) | 1.57 ± 0.40 (14) |
| 4 | 0 | 0 | 0 | 0 |

| Order | N |
|---|---|
| 4 | 9 |
| 3 | 22 |
| 2 | 19 |
| 1 | 30 |

N: Number of vessels studied for each order

**Table 2c**: connectivity matrix of pial arterioles in C14R group

| Order n | Order m | | | |
|---|---|---|---|---|
| | 1 | 2 | 3 | 4 |
| 0 | 2.22 ± 0.38 (69) | 0.25 ± 0.12 (4) | 0 | 0 |
| 1 | 0.33 ± 0.14 (10) | 0.52 ± 0.12 (9) | 0.28 ± 0.11 (7) | 0 |
| 2 | 0 | 0.28 ± 0.15 (5) | 1.24 ± 0.80 (30) | 0.66 ± 0.23 (7) |
| 3 | 0 | 0 | 0.29 ± 0.10 (7) | 1.33 ± 0.46 (15) |
| 4 | 0 | 0 | 0 | 0.33 ± 0.10 (4) |

| Order | N |
|---|---|
| 4 | 11 |
| 3 | 24 |
| 2 | 18 |
| 1 | 31 |

N: Number of vessels studied for each order

**Table 2d**: connectivity matrix of pial arterioles in C28R group

| Order n | Order m | | | |
|---|---|---|---|---|
| | 1 | 2 | 3 | 4 |
| 0 | 3.10 ± 0.72 (93) | 1.66 ± 0.14 (41) | 1.77 ± 0.25 (39) | 0 |
| 1 | 0.90 ± 0.19 (27) | 2.00 ± 0.18 (50) | 2.97 ± 0.15 (65) | 0.88 ± 0.56 (7) |
| 2 | 0 | 0.85 ± 0.15 (21) | 0.34 ± 0.10 (7) | 2.00 ± 0.23 (16) |
| 3 | 0 | 0 | 0.38 ± 0.07 (8) | 0.75 ± 0.13 (6) |
| 4 | 0 | 0 | 0 | 0 |

| Order | N |
|---|---|
| 4 | 8 |
| 3 | 22 |
| 2 | 25 |
| 1 | 30 |

N: Number of vessels studied for each order

**Table 2e**: connectivity matrix of pial arterioles in BMSCs7R group

| Order n | Order m | | | |
|---|---|---|---|---|
| | **1** | **2** | **3** | **4** |
| 0 | 4.35 ± 0.32 (152) | 1.60 ± 0.78 (43) | 0 | 0 |
| 1 | 0.76 ± 0.12 (27) | 3.80 ± 0.33 (103) | 3.05 ± 0.90 (70) | 0.95 ± 0.33 (9) |
| 2 | 0 | 1.13 ± 0.85 (31) | 4.52 ± 0.24 (104) | 2.10 ± 0.34 (19) |
| 3 | 0 | 0 | 0.50 ± 0.18 (12) | 1.98 ± 0.26 (18) |
| 4 | 0 | 0 | 0 | 0 |

| Order | N |
|---|---|
| 4 | 9 |
| 3 | 23 |
| 2 | 27 |
| 1 | 35 |

N: Number of vessels studied for each order

**Table 2f**: connectivity matrix of pial arterioles in BMSCs14R group

| Order n | Order m | | | |
|---|---|---|---|---|
| | **1** | **2** | **3** | **4** |
| 0 | 5.15 ± 0.18 (216) | 4.20 ± 0.55 (126) | 0 | 0 |
| 1 | 2.37 ± 0.60 (100) | 2.95 ± 0.88 (89) | 2.62 ± 0.37 (73) | 1.25 ± 0.13 (13) |
| 2 | 0 | 1.93 ± 0.25 (58) | 1.50 ± 0.95 (42) | 4.70 ± 0.25 (47) |
| 3 | 0 | 0 | 1.76 ± 0.43 (49) | 1.57 ± 0.30 (16) |
| 4 | 0 | 0 | 0 | 0.21 ± 0.08 (2) |

| Order | N |
|---|---|
| 4 | 10 |
| 3 | 28 |
| 2 | 30 |
| 1 | 42 |

N: Number of vessels studied for each order

**Table 2g**: connectivity matrix of pial arterioles in BMSCs28R group

| Group | Microvascular permeability (NGL) | Leukocyte Adhesion (Number of leukocytes/100 µm of venular length/30s) | Capillary perfusion (cm-1) |
|---|---|---|---|
| **S** | 0.02 ± 0.01 | 1.0 ± 0.5 | 106.0 ± 2.3 |
| **C1Hr** | 0.62 ± 0.03 ° | 10.0 ± 0.5 ° | 62.0 ± 1.4 ° |
| **C7R** | 0.47 ± 0.02 ° | 8.0 ± 0.5 ° | 67.0± 1.0 ° |
| **C14R** | 0.40 ± 0.03 ° | 6.0 ± 0.5 ° | 70.0 ± 1.4 ° |
| **C28R** | 0.20 ± 0.02° | 3.0 ± 0.2 ° | 85.1 ± 1.2 ° |
| **BMSCs7R** | 0.26 ± 0.03° | 4.0 ± 0.3 ° | 78 ± 1.5 ° |
| **BMSCs14R** | 0.18 ± 0.04° | 3.0 ± 0.4 ° | 90 ± 1.2 ° |
| **BMSCs28R** | 0.06 ± 0.03° | 0.9 ± 0.8 ° | 123 ± 1.8 ° |

**Table 3.** Summary of the principal parameters in sham-operated (*S*) group, in rats subjected to 2 hours of MCAO and 1h, 7 days, or 14 days or 28 days of reperfusion (C1hR, C7R, C14R and C28R group, respectively) and in rats underwent to 2 hours of MCAO plus BMSCs and 7, 14, 28 days of reperfusion (BMSCs7R, BMSCs14R, BMSCs28R group, respectively).
Capillary perfusion is expressed as $cm^{-1}$. NGL: Normalized Grey Levels. Leukocyte adhesion, expressed as number of adherent leukocytes to 100 µm of venular length for 30 s.
°$p<0.01$ vs. *S* group.

### *4.4 VEGF, eNOS, nNOS and iNOS expression*

To assess the role played by VEGF and the three different NOS proteins present in the brain of treated rats, their expression was evaluated in the ipsilesional (IPSI) temporoparietal cortex and striatum of rats subjected to MCAO plus BMSCs at different reperfusion time intervals: 7, 14 and 28 days, and compared with the expression of the same proteins in not treated rats.

We found that VEGF protein peaked on day 7 in the IPSI cortex and striatum, while on day 14 and 28 there was a decrease (Fig. 5). The same trend of the other proteins studied (e-NOS, p-eNOS, n-NOS and i-NOS) was detected (Fig 4, 6).

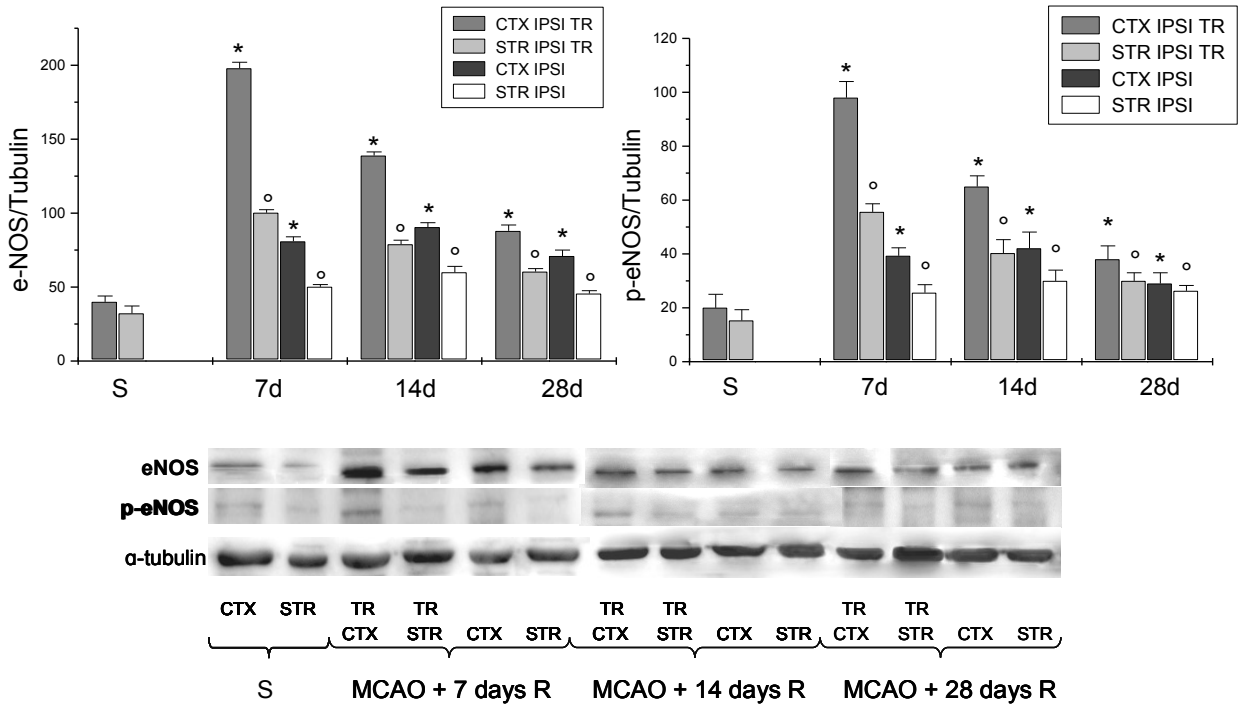


**Figure 4:** Western blotting of eNOS and phosphorilated eNOS expression in the cortex and striatum of sham-operated (CTX and STR), ischemic animals (CTX and STR) and of treated animals (TR CTX and TR STR); the corresponding densitometric values (mean ± SEM), expressed as arbitrary units calculated for each experimental group, were normalized on the basis of the respective α-tubulin. Each single experiment was repeated three times.* $p<0.01$ versus S and respective ischemic group in cortex. ° $p<0.01$ versus S and respective ischemic group in striatum.

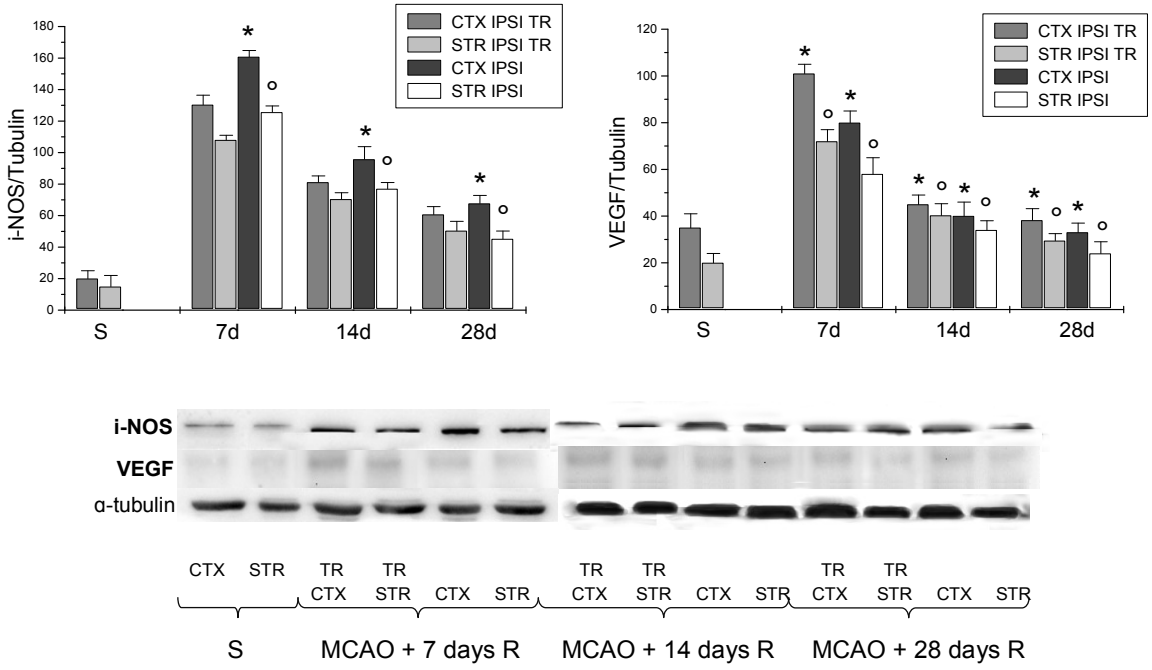


**Figure 5:**Western blotting of i-NOS and VEGF expression in the cortex and striatum of sham-operated (CTX and STR), ischemic animals (CTX and STR) and of treated animals (TR CTX and TR STR); the corresponding densitometric values (mean ± SEM), expressed as arbitrary units calculated for each experimental group, were normalized on the basis of the respective α-tubulin. Each single experiment was repeated three times. .* $p<0.01$ versus S and respective ischemic group in cortex. ° $p<0.012$ versus S and respective ischemic group in striatum.

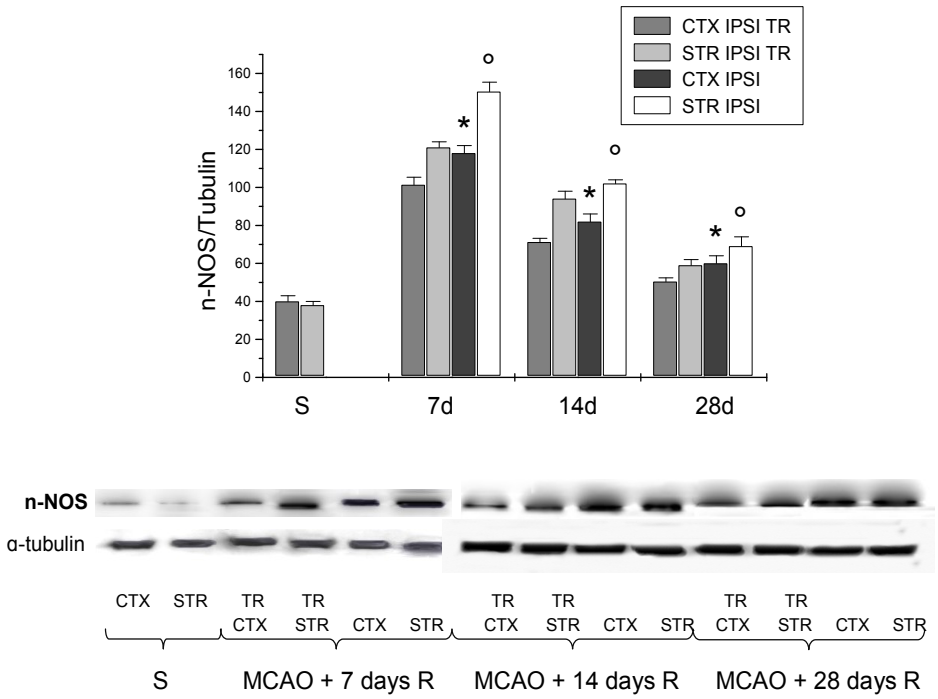


**Figure 6:**Western blotting of n-NOS expression in the cortex and striatum of sham-operated (CTX and STR), ischemic animals (CTX and STR) and of treated animals (TR CTX and TR STR); the corresponding densitometric values (mean ± SEM), expressed as arbitrary units calculated for each experimental group, were normalized on the basis of the respective α-tubulin. Each single experiment was repeated three times. .* $p<0.011$ versus S and respective ischemic group in cortex. ° $p<0.01$ versus S and respective ischemic group in striatum.

### *4.5 GFP-BMSCs distribution in infarcted area*

At seven days from GFP-BMSCs injection, into the infarcted area, a lot of these cells were distributed at random (Fig. 7A). After fourteen days of reperfusion these cells increased in number and were organized to form straight lines, in parallel to viable vessels (Fig. 7B). In the last group treated with these cells, after twenty-eight days of reperfusion, a reduced number of cells was observed into the interstitium compared to the previous group.

However it is worth noting, fluorescence was detected along the vessel walls (Fig. 7C). It was possible to observe, at higher magnification, the presence of GFP mesenchymal stem cells into the vessel walls (Fig. 7D).

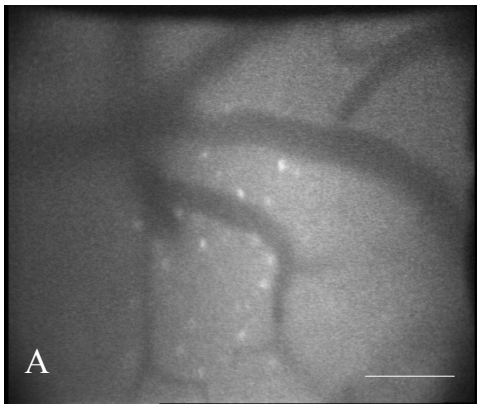
A

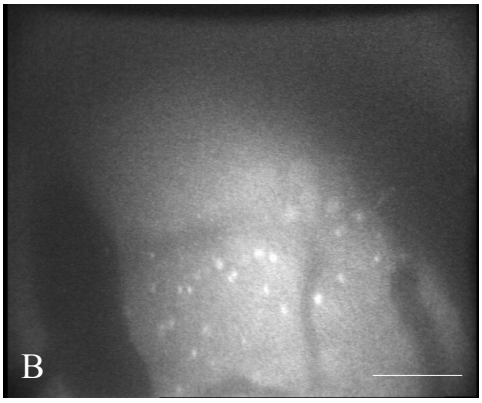
B

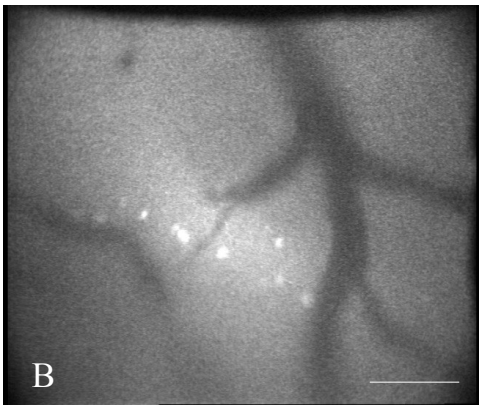
B

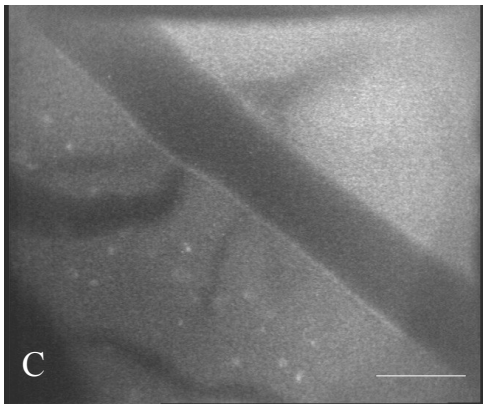
C

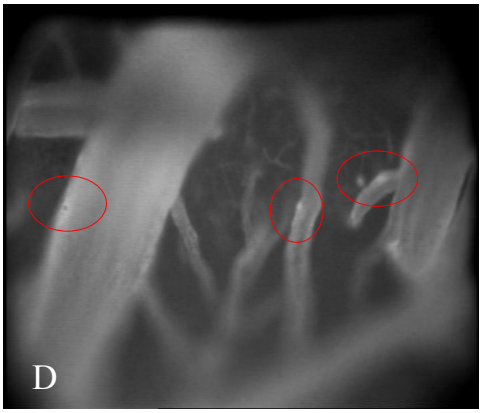
D

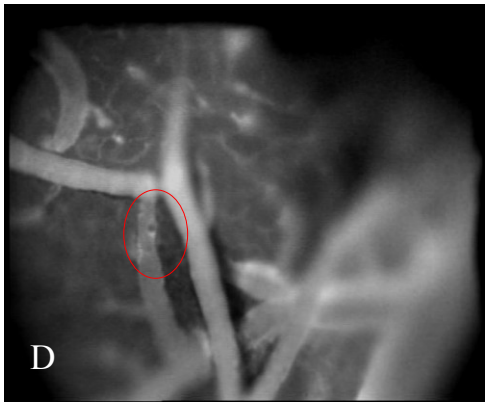
D

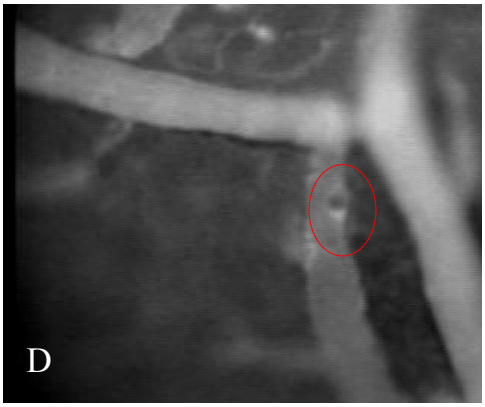
D

**Figure 7:** Computer-assisted image of GFP-BMSCs in infarcted area of rat pial microvascular network after MCAO and 7 days (A), 14 days (B) and 28 days of reperfusion (C, D).
Scale bar = _____ 100 μm.

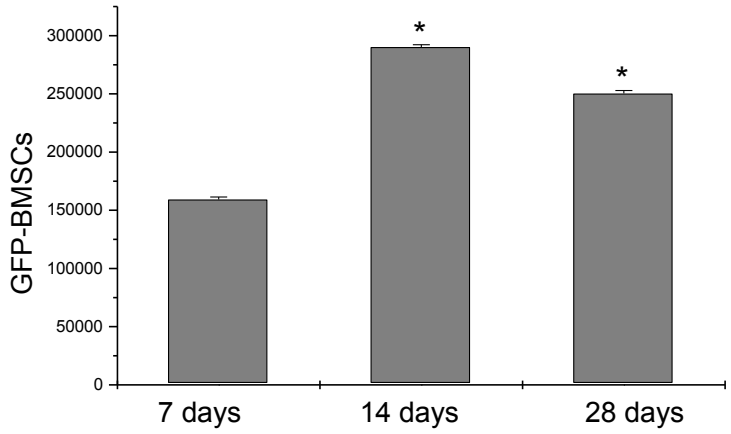


**Table 4:** Quantitative distribution of GFP-BMSCs in infarcted area after 7, 14 and 28 days of reperfusion. *p<0.01 vs GFP-BMSCs7R, °p<0.01 vs GFP-BMSCs14R.

## *4.6 Neurological assessment*

No significant differences in the behavioural tests were detected among the experimental groups before MCAO; the score was 0 (normal). Increasing the reperfusion time all treated animals showed a progressive decrease in behavioural deficits compared to ischemic animals. BMSCs28R group recovered from neurological damage: the score was 1.0 ± 0.5 (mild injury; p<0.01 vs. baseline conditions), (Fig. 8).

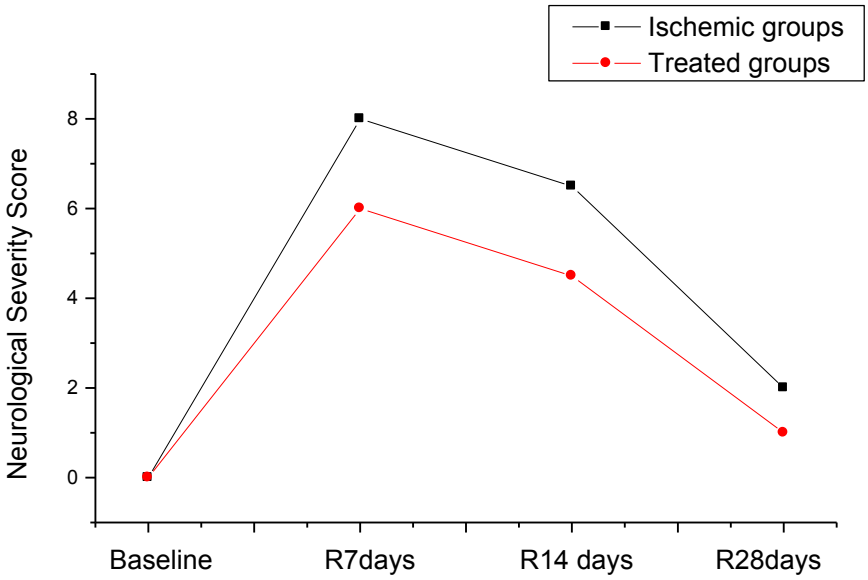


**Figure 8:** Neurological severity score of ischemic and treated animals

# 5. DISCUSSION AND CONCLUSIONS

The results of the present study indicate the post-ischemic penumbra induced by MCAO is a site of intense microvascular reorganization, characterized by new vessel connections resulting in several anastomotic arterioles.

MCAO for two hours and subsequent reperfusion for one hour caused an ischemic zone devoid of vessels, while the penumbra area presented few arterioles, capillaries, larger venules and marked microvascular permeability as well as marked leukocyte adhesion. These results are in accord with the observations by del Zoppo [59], because immediate events include breakdown of the primary endothelial cell barrier, plasma leakage and expression of endothelial cell leukocyte adhesion receptors.

After 7 and 14 days of reperfusion, perfused arterioles progressively increased in number, showing a different geometric arrangement. Connectivity matrix indicates parent vessels were connected to smaller arterioles than in S group, characterized by order n+1 arterioles giving origin to most order n arterioles. In ischemic animals until twenty-eight days of reperfusion parent vessels were not connected with (a majority of) daughter vessels of immediately successive order; therefore, an order gap was observed, i.e. predominant connections of the largest with the smallest arterioles. Moreover, vessel branchings in ischemic animals were not the same as in sham-operated group.

It is reasonable to suggest that the increase in number of perfused arterioles at seven days of reperfusion give origin to new branchings with vessel formation and connections, as suggested by anastomotic arterioles appearing after seven days and increasing in number at fourteen days of reperfusion. These vessels constituted arteriolar arcades overlapping and supplying blood to ischemic core. Vascular remodeling was complex and involved vessel adjustment in length and branchings until twenty-eight days of reperfusion.

The intracarotid administration of bone mesenchymal stem cells post middle cerebral artery occlusion induced an accelerated pial vascular remodeling.

We could compare the geometric reorganization of arteriolar networks in treated and not treated groups; moreover we compared treated group after 7 days of reperfusion with the ischemic group after 14 days of reperfusion. At 14 days of reperfusion we detected the same geometric characteristics observed after 28 days of reperfusion in not treated group. We could suggest that the role of these cells was to anticipate the remodeling processes of pial networks, because at 7 days of reperfusion in treated groups

we have the same microvascular arrangement as in not treated groups after 14 days. A pronounced number, indeed, of anastomotic arcading arterioles characterized the pial microvasculature. These arcades were likely vessels sprouting from preexistent arterioles localized in the penumbra area, able to overlap the ischemic core. Comparing the connectivity matrix obtained from the different experimental preparation, we noticed in the treated groups that arterioles of *n+1* order give origin to most anastomotic vessel of order *n*.

VEGF, the most important mitogen in the process of angiogenesis, promotes the vascular remodelling. We show that BMSCs increase the expression of this protein and induce the other protein expression playing an important role in the mechanism of remodelling.

eNOS and p-eNOS expression peaked after 7 days of reperfusion the expression. Conversely, the inducible NOS expression decreased; this effect induced by transplantation cells cause reduced expression of inflammatory factors helping to minimize post-ischemic inflammation and ischemic damage in the host brain [60].

nNOS was induced and activated in penumbra and core during acute phase of experimental stroke [26]; the long-lasting production of NO might induce neurotoxic damage. Previous data indicated that the infarct volume after experimental stroke decreased significantly in nNOS gene knockout or nNOS inhibition [61, 62]. Our data, indeed, show that nNOS expression in cortex and striatum was reduced by treatment of BMSCs. Therefore, BMSCs can provide a resource of several trophic and growth factors, playing important roles in angiogenesis and stimulating differentiation of BMSCs [63].

GFP-BMSCs were useful to show the distribution and the organization of these cells into the infarcted area. More GFP-BMSCs were found in the lesioned hemisphere after 7 days. Distruption of the blood-brain barrier after MCAO may facilitate selective entry of BMSCs into ischemic brain compared with nonischemic contralateral hemisphere [58]. After fourteen days these cells were organized in penumbra area to form straight lines, suggesting a model for vessel tube formation. In the last group of treated animals with GFP-BMSCs, after 28 days we observed marked fluorescence along the vessel walls and a reduced number of cells into the penumbra area. Therefore, the role of these cells into the vessels might be flowmotion of linear sprouting of new branching was fundamental to contribute to remodeling processe acceleration.

This was accompanied by behavioural data from the battery of functional tests demonstrating that motor and sensory functions progressively recovered after ischemic insult. Significantly better performances were detected at 28 days of reperfusion after BMSCs injection. Therefore, neuronal recovery accompanied vascular remodelling.

In conclusion, pial vascular remodeling after transient middle cerebral artery occlusion mainly involves arteriolar networks. The graft of bone mesenchymal stem cells accelerate these processes. An increasing number of anastomotic arcading arterioles characterize pial microvasculature. These arcades were likely vessels sprouting from preexistent arterioles localized in the penumbra area, able to overlap the ischemic core.

Accelerate remodeling mechanisms appeared accompained by higher expression of VEGF and eNOS likely modulating angiogenesis *in vivo*. Finally, cerebral microvessels remodeling was accompanied by improved neurological behaviour.

# 6. References


1. Adina Michael-Titus, Patricia Revest, Peter Shortland: The Nervous System. Churchill Livingstone ELSEVIER.
2. Rosamond W, Flegal K, Friday G, Furie K, Go A, Greenlund K, Haase N, Ho M, Howard V, Kissela B, Kittner S, Lloyd-Jones D, McDermott M, Meigs J, Moy C, Nichol G, O'Donnell CJ, Roger V, Rumsfeld J, Sorlie P, Steinberger J, Thom T, Wasserthiel-Smoller S, Hong Y, American Heart Association Statistics Committee and Stroke Statistics Subcommittee: Heart disease and stroke statistics-2007 update: a report from the American heart association statistics committee and stroke statistics subcommittee. *Circulation* 2007, **115:**e69–e171
3. Dirnagl U, Iadecola C, Moskowitz MA: Pathobiology of ischaemic stroke: an integrated view. *Trends Neurosci* 1999, 22:391–397.].
4. Hossmann K-A: Pathophysiology and therapy of experimental stroke**.** *Cel Mol Neurobiol* 2006, **26:**1055–1081
5. Richard Green A, Odergren T, Ashwood T: Animal models of stroke: do they have value for discovering neuroprotective agents? *Trends Pharmacol Sci* 2003, 24:402–408
6. Hacke et al., 2008 Thrombolysis for acute stroke under antiplatelet therapy: safe enough to be beneficial.
7. Wang X, Lo EH. Triggers and mediators of hemorrhagic transformation in cerebral ischemia. Mol Neurobiol. 2003 Dec;28(3):229-44.
8. Gutiérrez M, Merino JJ, de Leciñana MA, Díez-Tejedor E. Cerebral protection, brain repair, plasticity and cell therapy in ischemic stroke. Cerebrovasc Dis. 2009;27 Suppl 1:177-86. doi: 10.1159/000200457. Epub 2009 Apr 3.
9. Chopp M, Li Y. Treatment of neural injury with marrow stromal cells. Lancet Neurol. 2002 Jun;1(2):92-100.
10. Prockop DJ, Azizi SA, Phinney DG, Kopen GC, Schwarz EJ. Potential use of marrow stromal cells as therapeutic vectors for diseases of the central nervous system. Prog Brain Res. 2000;128:293-7.

11. N. Joyce, G. Annett, L.Wirthlin, S. Olson, G. Bauer, J.A. Nolta, Mesenchymal stem cells for the treatment of neurodegenerative disease, Regen. Med. 5 (6) (2010) 933–946.
12. L.R. Zhao,W.M. Duan, M. Reyes, C.D. Keene, C.M. Verfaillie,W.C. Low, Human bone marrow stem cells exhibit neural phenotypes and ameliorate neurological deficits after grafting into the ischemic brain of rats, Exp. Neurol. 174 (1) (2002) 11–20.
13. Y. Takagi, M. Nishimura, A. Morizane, J. Takahashi, K. Nozaki, J. Hayashi, N. Hashimoto, Survival and differentiation of neural progenitor cells derived from embryonic stem cells and transplanted into ischemic brain, J. Neurosurg. 103 (2) (2005) 304–310.
14. L. Crigler, R.C. Robey, A. Asawachaicharn, D. Gaupp, D.G. Phinney, Human mesenchymal stem cell subpopulations express a variety of neuro-regulatory molecules and promote neuronal cell survival and neuritogenesis, Exp. Neurol. 198 (1) (2006) 54–64.
15. I. Aizman, C.C. Tate, M. McGrogan, C.C. Case, Extracellular matrix produced by bone marrow stromal cells and by their derivative, SB623 cells, supports neural cell growth, J. Neurosci. Res. 87 (14) (2009) 3198–3206.
16. H.J. Kim, E. McMillan, F. Han, C.N. Svendsen, Regionally specified human neural progenitor cells derived from the mesencephalon and forebrain undergo increased neurogenesis following overexpression of ASCL1, Stem Cells 27 (2) (2009) 390–398.
17. J. Sharp, H.S. Keirstead, Stem cell-based cell replacement strategies for the central nervous system, Neurosci. Lett. 456 (3) (2009) 107–111.
18. L. Danielyan, R. Schafer, A. von Ameln-Mayerhofer, M. Buadze, J. Geisler, T. Klopfer, U. Burkhardt, B. Proksch, S. Verleysdonk, M. Ayturan, G.H. Buniatian, C.H. Gleiter, W.H. Frey 2nd, Intranasal delivery of cells to the brain, Eur. J. Cell Biol. 88 (6) (2009) 315–324.
19. J.R. Munoz, B.R. Stoutenger, A.P. Robinson, J.L. Spees, D.J. Prockop, Human stem/progenitor cells from bone marrow promote neurogenesis of endogenous neural stem cells in the hippocampus of mice, Proc. Natl. Acad. Sci. U. S. A. 102(50) (2005) 18171–18176.

20. Conti L, Cataudella T, Cattaneo E (2003) Neural stem cells: a pharmacological tool for brain diseases? Pharmacol Res 47:289–297.
21. Savitz SI, Chopp M, Deans R, Carmichael ST, Phinney D, Wechsler L (2011) Stem cell therapy as an emerging paradigm for stroke (STEPS) II. Stroke 42:825–829.
22. Qi X, Shao M, Peng H, Bi Z, Su Z, Li H (2010) In vitro differentiation of bone marrow stromal cells into neurons and glial cells and differential protein expression in a two-compartment bone marrow stromal cell/neuron co-culture system. J Clin Neurosci 17:908–913.
23. Shichinohe H, Kuroda S, Maruichi K, Osanai T, Sugiyama T, Chiba Y, Yamaguchi A, Iwasaki Y (2010) Bone marrow stromal cells and bone marrow-derived mononuclear cells: which are suitable as cell source of transplantation for mice infarct brain? Neuropathology 30:113–122.
24. Shen LH, Li Y, Chen J, Cui Y, Zhang C, Kapke A, Lu M, Savant-Bhonsale S, Chopp M (2007) One-year follow-up after bone marrow stromal cell treatment in middle-aged female rats with stroke. Stroke 38:2150–2156.
25. J. van Gijn, M.S. Dennis, Issues and answers in stroke care, Lancet 352 (Suppl. 3) (1998) SIII23–SIII27.
26. M. Hayase, M. Kitada, S. Wakao, Y. Itokazu, K. Nozaki, N. Hashimoto, Y. Takagi, M. Dezawa, Committed neural progenitor cells derived from genetically modified bone marrow stromal cells ameliorate deficits in a rat model of stroke, J. Cereb. Blood Flow Metab. 29 (8) (2009) 1409–1420.
27. J. Chen, Y. Li, L. Wang, Z. Zhang, D. Lu, M. Lu, M. Chopp, Therapeutic benefit of intravenous administration of bone marrow stromal cells after cerebral ischemia in rats, Stroke 32 (4) (2001) 1005–1011.
28. M.A. Eglitis, D. Dawson, K.W. Park, M.M. Mouradian, Targeting of marrow-derived astrocytes to the ischemic brain, Neuroreport 10 (6) (1999) 1289–1292.
29. K. Kurozumi, K. Nakamura, T. Tamiya, Y. Kawano, M. Kobune, S. Hirai, H. Uchida, K. Sasaki, Y. Ito, K. Kato, O. Honmou, K. Houkin, I. Date, H. Hamada, BDNF gene-modified mesenchymal stem cells promote functional recovery and reduce infarct size in the rat middle cerebral artery occlusion model, Mol. Ther. 9 (2) (2004) 189–197.

30. N. Ikeda, N. Nonoguchi, M.Z. Zhao, T. Watanabe, Y. Kajimoto, D. Furutama, F. Kimura, M. Dezawa, R.S. Coffin, Y. Otsuki, T. Kuroiwa, S. Miyatake, Bone marrow stromal cells that enhanced fibroblast growth factor-2 secretion by herpes simplex virus vector improve neurological outcome after transient focal cerebral ischemia in rats, Stroke 36 (12) (2005) 2725–2730.
31. J. Chen, Y. Li, M. Chopp, Intracerebral transplantation of bone marrow with BDNF after MCAo in rat, Neuropharmacology 39 (5) (2000) 711–716.
32. Y. Li, J. Chen, X.G. Chen, L.Wang, S.C. Gautam, Y.X. Xu, M. Katakowski, L.J. Zhang,M. Lu, N. Janakiraman, M. Chopp, Human marrow stromal cell therapy for stroke in rat: neurotrophins and functional recovery, Neurology 59 (4) (2002) 514–523.
33. J. Chen, Z.G. Zhang, Y. Li, L.Wang, Y.X. Xu, S.C. Gautam,M. Lu, Z. Zhu,M. Chopp, Intravenous administration of human bonemarrowstromal cells induces angiogenesis in the ischemic boundary zone after stroke in rats, Circ. Res. 92 (6) (2003) 692–699.
34. Gibbons GH, Dzau VJ: The emerging concept of vascular remodeling. N Engl J Med 1994;330:1431-1438.
35. Wagner S, Tagaya M, Koziol JA, Quaranta V, del Zoppo GJ: Rapid disruption of an astrocyte interaction with the extracellular matrix mediated by integrin $\alpha_6\beta_4$ during focal cerebral ischemia/reperfusion. Stroke 1997;28:858-865.
36. Cipolla MJ, Lessov N, Hammer ES, Curry AB: Threshold duration of ischemia for myogenic tone in middle cerebral arteries: effect on vascular smooth muscle actin. Stroke 2001;32:1658-1664.
37. Mostany R, Chowdhury TG, Johnston DG, Portonovo SA, Carmichael ST, Portera-Cailliau C: Local hemodynamics dictate long-term dendritic plasticity in peri-infarct cortex. J Neurosci 2010;30:14116-14126.
38. Li Y, Chen J, Chen XG, Wang L, Gautam SC, Xu YX, Katakowski M, Zhang LJ, Lu M, Janakiraman N, Chopp M. Human marrow stromal cell therapy for stroke in rat: neurotrophins and functional recovery. *Neurology*. 2002;59:514 –523; Wu J, et al 2008 Cell Transplant.

39. Komatsu K, Honmou O, Suzuki J, Houkin K, Hamada H, Kocsis JD. Therapeutic time window of mesenchymal stem cells derived from bone marrow after cerebral ischemia. Brain Res. 2010 Jun 2;1334:84-92.
40. Chavakis E, Urbich C, Dimmeler S. Homing and engraftment of progenitor cells: a prerequisite for cell therapy. J Mol Cell Cardiol. 2008 Oct;45(4):514-22.
41. Honma T, Honmou O, Iihoshi S, Harada K, Houkin K, Hamada H, Kocsis JD. Intravenous infusion of immortalized human mesenchymal stem cells protects against injury in a cerebral ischemia model in adult rat. Exp Neurol. 2006 May;199(1):56-66.
42. Di Nicola M, Carlo-Stella C, Magni M, Milanesi M, Longoni PD, Matteucci P, Grisanti S, Gianni AM. Human bone marrow stromal cells suppress T-lymphocyte proliferation induced by cellular or nonspecific mitogenic stimuli. Blood 2002; 99: 3838–43.
43. Qi X, Shao M, Peng H, Bi Z, Su Z, Li H (2010) In vitro differentiation of bone marrow stromal cells into neurons and glial cells and differential protein expression in a two-compartment bone marrow stromal cell/neuron co-culture system. J Clin Neurosci 17:908–913 ;
44. Shichinohe H, Kuroda S, Maruichi K, Osanai T, Sugiyama T, Chiba Y, Yamaguchi A, Iwasaki Y (2010) Bone marrow stromal cells and bone marrow-derived mononuclear cells: which are suitable as cell source of transplantation for mice infarct brain? Neuropathology 30:113–122
45. Shen LH, Li Y, Chen J, Cui Y, Zhang C, Kapke A, Lu M, Savant-Bhonsale S, Chopp M (2007) One-year follow-up after bone marrow stromal cell treatment in middle-aged female rats with stroke. Stroke 38:2150–2156.
46. Oswald J, Boxberger S, Jorgensen B, Feldmann S, Ehninger G, Bornhauser M, Werner C. Mesenchymal stem cells can be differentiated into endothelial cells in vitro. *Stem Cells* 2004; 22: 377-84.
47. Kinnaird T, Stabile E, BurnettMS, Shou M, Lee CW, Barr S, Fuchs S, Epstein SE. Local delivery of marrow-derived stromal cells augments collateral perfusion through paracrine mechanisms. Circulation 2004;109: 1543–49.

48. Kroll J, Waltenberger J: VEGF-A induces expression of eNOS and iNOS in endothelial cells via VEGF receptor-2 (KDR). Biochem Biophys Res Commun 1998;252:743-746.
49. Lee JB, Kuroda S, Shichinohe H *et al*. A pre-clinical assessment model of rat autogeneic bone marrow stromal cell transplantation into the central nervous system. *Brain Res Brain Res Protoc* 2004; **14**: 37–44.
50. Sugiyama T, Kuroda S, Osanai T *et al*. Near-infrared fluorescence labeling allows noninvasive tracking of bone marrow stromal cells transplanted into rat infarct brain. *Neurosurgery* 2011; **68**: 1036–1047; discussion 47.
51. Lee JB, Kuroda S, Shichinohe H *et al*. Migration and differentiation of nuclear fluorescence-labeled bone marrow stromal cells after transplantation into cerebral infarct and spinal cord injury in mice. *Neuropathology* 2003; **23**: 169–180.
52. Shichinohe H, Kuroda S, Sugiyama T *et al*. Biological features of human bone marrow stromal cells (hBMSC) cultured with animal protein-free medium – safety and efficacy of clinical use for neurotransplantation. *Transl Stroke Res* 2011.
53. Longa EZ, Weinstein PR, Carlson S, Cummins R. Reversible middle cerebral artery occlusion without craniectomy in rats. Stroke 1989;20:84-91.
54. Ngai AC, Ko KR, Morii S, Winn HR: Effect of sciatic nerve stimulation on pial arterioles in rats. Am J Physiology Hearth and Circulation 1988;254:H133-H139.
55. Golanov EV, Yamamoto S, Reis DJ: Spontaneous waves of cerebral blood flow associated with a pattern of electrocortical activity. Am J Physiology 1994;266:R204-R214.
56. Kassab GS, Lin DH, Fung YC: Morphometry of pig coronary arterial trees. Am J Physiol, 1993; 256: H350-H365.
57. Lapi D, Marchiafava PL, Colantuoni A: Geometric Characteristics of arterial network of rat pial microcirculation. J Vasc Res 2008;45:69-77.
58. Chen J, Li Y, Wang L, Lu M, Zhang X, Chopp M: Therapeutic benefit of intravenous administration of bone marrow stromal cells after cerebral ischemia in rats. Stroke 2001;32:1005-1011.
59. del Zoppo GJ: Stroke and neurovascular protection. N Engl J Med 2006;354:553-555.

60. Ling Wei, Jamie L. Fraser, Zhong-Yang Lu, Xinyang Hu, Shan Ping Yu. Transplantation of hypoxia preconditioned bone marrow mesenchymal stem cells enhances angiogenesis and neurogenesis after cerebral ischemia in rats. Neurobiology of Disease 46 (2012) 635–645.
61. Samdani AF, Dawson TM, Dawson VL. Nitric Oxide Synthase in Models of Focal Ischemia. Stroke. 1997 Jun;28(6):1283-8.
62. Willmot M, Gibson C, Gray L, Murphy S, Bath P. Nitric oxide synthase inhibitors in experimental ischemic stroke and their effects on infarct size and cerebral blood flow: a systematic review. Free Radic Biol Med. 2005 Aug 1;39(3):412-25. Epub 2005 Apr 12.
63. Kurozumi K, Nakamura K, Tamiya T, Kawano Y, Ishii K, Kobune M, Hirai S, Uchida H, Sasaki K, Ito Y, Kato K, Honmou O, Houkin K, Date I, Hamada H. Mesenchymal stem cells that produce neurotrophic factors reduce ischemic damage in the rat middle cerebral artery occlusion model. Mol Ther. 2005 Jan;11(1):96-104.